



**Michigan
Technological
University**

Michigan Technological University
Digital Commons @ Michigan Tech

Dissertations, Master's Theses and Master's Reports

2016

EXPERIMENTAL STUDY OF THE FLOW OF FERROFLUID IN A POROUS MEDIA UNDER A MAGNETIC FIELD

Muskaan Khurana

Michigan Technological University, mkhurana@mtu.edu

Copyright 2016 Muskaan Khurana

Recommended Citation

Khurana, Muskaan, "EXPERIMENTAL STUDY OF THE FLOW OF FERROFLUID IN A POROUS MEDIA UNDER A MAGNETIC FIELD", Open Access Master's Thesis, Michigan Technological University, 2016.

<https://doi.org/10.37099/mtu.dc.etdr/238>

Follow this and additional works at: <https://digitalcommons.mtu.edu/etdr>



Part of the [Geology Commons](#), [Geophysics and Seismology Commons](#), [Heat Transfer, Combustion Commons](#), [Oil, Gas, and Energy Commons](#), and the [Water Resource Management Commons](#)

EXPERIMENTAL STUDY OF THE FLOW OF FERROFLUID IN A POROUS MEDIA UNDER A MAGNETIC FIELD

By

Muskaan Khurana

A THESIS

Submitted in partial fulfillment of the requirements for the degree of
MASTER OF SCIENCE

In Geophysics

MICHIGAN TECHNOLOGICAL UNIVERSITY

2016

©2016 Muskaan Khurana

This thesis has been approved in partial fulfillment of the requirements for the Degree of MASTER OF SCIENCE in Geophysics.

Department of Geological and Mining Engineering and Sciences

Thesis Co-Advisor: *Dr. Roohollah (Radwin) Askari*

Thesis Co-Advisor: *Dr. Ezequiel Medici*

Committee Member: *Dr. John S. Gierke*

Department Chair: *Dr. John S. Gierke*

Table of Contents

List of Figures.....	v
List of Tables.....	vii
Acknowledgements.....	viii
Abstract.....	ix
1. Introduction.....	1
1.1 Background and Motivation.....	1
1.2 Fluid Flow in Porous Media.....	4
1.3 Objectives.....	8
1.4 Analytical Model of Varying Magnetic Field with Distance.....	8
2. Methodology.....	12
2.1 Experimental Setup.....	12
2.2 Experimental Testing.....	14
2.2.1 Materials and Methods.....	14
2.2.2 Methods.....	17
2.2.3 Water Injection into an Air Saturated Medium.....	18
2.2.4 Water Injection into an Oil Saturated Medium.....	18
2.2.5 Oil Based Ferrofluid Injection into an Air Saturated Porous Medium.....	19
2.2.6 Oil Based Ferrofluid Displacing Oil from an Oil Saturated Medium.....	21
2.2.7 Water Based Ferrofluid Injection into an Air Saturated Medium.....	23
2.2.8 Water Based Ferrofluid Displacing Oil from an Oil Saturated Medium....	24
2.2.9 Table for Experiments Conducted.....	26
3. Image Post Processing and Data Analysis.....	27
3.1 Image Post Processing.....	27
3.2 Observations.....	28
3.2.1 Water Displacing Air.....	28

3.2.2	Water Displacing Oil.....	31
3.2.3	Oil Based Ferrofluid in an Air Saturated Medium.....	32
3.2.4	Water Based Ferrofluid in an Air Saturated Medium.....	34
3.2.5	Oil Based Ferrofluid in an Oil Saturated Medium	37
3.2.6	Oil Based Injection into a Ferrofluid with Magnetic Field in Vicinity.....	39
3.2.7	Water Based Ferrofluid Injection in an Oil Saturated Medium.....	40
4.	Summary and Conclusion.....	44
4.1	Summary	44
4.2	Conclusion.....	46
4.3	Future Work.....	48
5.	Bibliography.....	49

List of Figures

1.1	Drainage Phase Diagram.....	5
1.2	Magnetic Field Variation with Distance.....	11
1.3	Magnetic Bond Number Variation with Distance.....	11
2.1	Experimental Setup.....	13
2.2	Water Displacing Air at Pump Speeds Ultralow 1, 6, 10 and normal 4 respectively.....	18
2.3	Water Displacing at Pump Speeds Ultralow 1, 6, 10.....	19
2.4	Oil Based Ferrofluid Displacing Air with No Magnetic Field at Pump Speeds Ultralow 1, 6.....	20
2.5	Oil Based Ferrofluid Displacing Oil in the Vicinity of Magnet at Pump Speeds Ultralow 1, 6, 10.....	22
2.6	Oil Based Ferrofluid Displacing Oil with No Magnetic Field at Pump Speeds Ultralow 6, 10.....	23
2.7	Water Based Ferrofluid Displacing Air with No Magnetic Field at Pump Speeds Ultralow 1.....	23
2.8	Water Based Ferrofluid Displacing Air in the Vicinity of Magnet at Pump Speeds Ultralow 1, 6, 10.....	24
2.9	Water Based Ferrofluid Displacing Oil with Magnetic Field at Pump Speeds Ultralow 6, 10.....	25
2.10	Water Based Ferrofluid Displacing Oil at Pump Speeds Ultralow 1, 6, 10.....	26
3.1	Water Displacing Air at Flowrates U1 and U6.....	30
3.2	S Curve for Water Displacing Air at Flowrate U1.....	30
3.3	Water Displacing Oil at Flowrates U1 and U6.....	31
3.4	S Curve for Water Displacing Oil at Flowrate U1 and U6.....	32
3.5	Oil based ferrofluid displacing air without a magnetic field at the flowrates U1 and U6.....	33
3.6	S Curve for Oil based ferrofluid displacing air without a magnetic field at flowrates U1 and U6.....	33
3.7	Water based ferrofluid displacing air without a magnetic field at the flowrates U1 and U6.....	35
3.8	S Curve for Water based ferrofluid displacing air without a magnetic field at flowrates U1 and U6.....	35

3.9	Water based ferrofluid displacing air with a magnetic field in vicinity at the flowrates U1 and U6.....	36
3.10	S Curve for Water based ferrofluid displacing air with a magnetic field in vicinity at flowrates U1 and U6.....	37
3.11	Oil based ferrofluid displacing oil without a magnetic field at the flowrates U1 and U6.....	38
3.12	S Curve for Oil based ferrofluid displacing oil without a magnetic field at flowrates U1 and U6.....	38
3.13	Oil based ferrofluid displacing oil with a magnetic field in vicinity at the flowrates U1 and U6.....	40
3.14	S Curve for Oil based ferrofluid displacing oil with a magnetic field in vicinity at flowrates U1 and U6.....	40
3.15	Water based ferrofluid displacing oil without a magnetic field at the flowrates U1 and U6.....	41
3.16	S Curve for Water based ferrofluid displacing oil without a magnetic field in vicinity at flowrates U1 and U6.....	41
3.17	Water based ferrofluid displacing oil with a magnetic field at the flowrates U1 and U6.....	42
3.18	S Curve for Water based ferrofluid displacing oil with a magnetic field in vicinity at flowrates U1 and U6.....	43
4.1	Perimeter vs Time curve for ferrofluid injection into an Oil satu-rated medium at flow rates 126microlitres/min and 23.4 micro-liters/min (U1 and U6 respectively) with or without the magnetic field in vicinity.....	47
4.2	Perimeter vs Time curve for ferrofluid injection into an air satu-rated medium at flow rates 126microlitres/min and 23.4 micro-liters/min (U1 and U6 respectively) with or without the magnetic field in vicinity.....	48

List of Tables

2.1	Ferrofluid EFH1.....	15
2.2	Ferrofluid EMG 308.....	15
2.3	Specification of Neodymium magnet – N45.....	16
2.4	Motor Oil Sw – 33.....	16
2.5	Water Properties.....	17
2.6	List of Experiments.....	26

Acknowledgement

I would like to express my deepest gratitude to my advisor Professor Roohollah Askari, who gave me continued guidance and support at all times. My deepest appreciation goes to Dr. Ezequiel Medici, without his guidance and persistent help this thesis wouldn't have been possible.

In addition, I would like to whole heartedly thank my friends Devak, Sameer, Avi, Prakirti, Kishan and Nupur for all the help and support, and most importantly my parents and brother for motivating me through hard times, without you guys I wouldn't have been able to make it this far.

Abstract

This research presents results from a laboratory-scale experimental setup that was designed to visualize the behavior of ferrofluid percolation through a porous media. Ferrofluids are colloidal suspensions made of magnetic particles of a few nanometers and stabilized in carrier liquids like water or mineral oil. Ferrofluids get magnetized and align themselves in the direction of a magnetic field when a field gradient is applied.

With the help of this experiment we investigate the viability of controlling fluid flow in porous medium by a magnetic field in vicinity. The experiments show that ferrofluids can be used as a transporting media to push the higher viscosity fluid out of the porous media when magnetic forces are acting on it. The magnetic force produces stronger attractive forces on the ferrofluid around the magnet which results in a predictable arrangement which is independent of the heterogeneity of the medium. When capillary or viscous forces are predominant during the 2-dimensional drainage of immiscible fluids in a permeable medium, the injected fluid forms very thin finger like structure which then retains the fluid being displaced in them. No fingers due to varying viscosities are observed during displacement by ferrofluids in the medium. Displacement visualization experiments in an oil saturated porous medium shows that ferrofluids obtain a rectangular shaped final configuration around the magnet, irrespective of the initial arrangement and flow path. The aim of this research is to control the instabilities that occur during the displacement of a fluid with the help of ferrofluid and magnetic field in vicinity.

While the applications of ferrofluids are promising in the field of engineering, the results obtained are particularly relevant to the laboratory scale experiments where the weakening of magnetic strength due to increasing distance is a smaller limitation. Ferrofluids may find an immediate application in areas like enhancing oil recovery, in environmental engineering that requires maneuvering subsurface liquids in the field, treatment. Their properties could also be utilized in a situation that requires controlling the emplacement of fluid motion, guiding to or positioning to target zones in the subsurface without coming in direct access with it.

Chapter 1

Introduction

1.1 Background and Motivation

Different materials respond differently to external magnetic fields. Susceptibility is an instructive way to find out about the dependency of these materials on applied magnetic fields. There are four different types of magnetic materials. Diamagnetic materials have paired number of electrons in an atom. Hence there is no net magnetic moment observed when a magnetic field is applied. The susceptibility of diamagnetic particles is small and negative which means the magnetization induced is opposite the applied magnetic field. Paramagnetism occurs when the atoms of a substance have a positive magnetic susceptibility due to unpaired electrons that align themselves in the direction of an applied field. Atoms of a paramagnetic material have randomly oriented magnetic moments. Ferromagnetism alludes to materials such as iron and nickel. The electrons for these materials create a small magnetic field when they spin and orbit around the nucleus of an atom. When an external magnetic field is present, the unpaired electrons line up parallel to each other while spinning in an area named as domain where the intensity of magnetic field is high[21]. There are a lot of crystalline materials which exhibit ferromagnetism, like iron (Fe), Cobalt (Co), Nickel (Ni) etc. Ferrimagnetism is observed in ionic compounds which have more complex crystal structure, such as Magnetite (Fe_3O_4) etc. The alignment of atoms due to interactions within the material leads to parallel alignment in some of the crystal sites and anti-parallel in other. The only difference between ferromagnetic and ferrimagnetic material is the saturation magnetization. Ferrimagnetic materials behave similar to ferromagnetic just that their saturation magnetization is lower.

Ferrofluids are colloidal suspensions of magnetite (Ferrimagnetic mineral and the naturally occurring oxides of iron with a chemical formula of $(\text{Fe}_3 \text{O}_4)$) material suspended in a carrier and are separated by a dispersant, which is generally a surface active substance added to a colloidal suspension to prevent clumping. In the presence of a magnetic field, the single domain small colloidal particles become magnetized.

The small size of the ferrofluids enables them to flow through a porous media, which are characterized by division of the total volume into solid matrix and pore space, with the pore space being occupied by one or more fluids [8]. Examples of the latter could be Styrofoam, sediments and fractured rocks. On the application of large magnetic field gradient, the ferrofluids flow toward regions of stronger magnetic field, which can further help alter the hydrodynamic properties of the fluid such as viscosity, surface tension which is the contact angle of fluids on surfaces and can alter the behavior and shape of the ferrofluid droplets (Butter et al, 2003; Dababneh & Ayoub, 1993; Nguyen et al 2010; Ody et al 2016; Zhou, et al 2011; Zhu et al 2011). The contact angle of a ferrofluid droplet changes with the application of a magnetic field. In the absence of magnetic field, the contact angle varies between 72° - 90° , while under a magnetic field, the droplet flattens and the contact angle varies from 180° - 200° . The attractive magnetic forces generated between a ferrofluid and an external magnetic field allows it to flow in the desired direction[1]. This effect can be potentially engineered to gain better insight of the behavior of ferrofluids in porous media and to quantify if their displacement can be controlled with the help of an external magnetic field. Further, to increase the understanding of ferrofluid displacement in fluid saturated medium, the possibility of controlling the formation of irregular fingers by viscosity and flow variations is explored. The advantage of doing micro level fluid flow study of ferrofluid flow in a porous media is enticing, because there is no direct contact with the fluid [3].

The potential for this technology to stabilize the irregular fingering in oil recovery is motivating and has been further discussed in the thesis. There are number of Enhanced Oil recovery (EOR) techniques used currently. Each of them have implications on cost, efficiency and safety. Oil production is broken down into three phases, primary, Secondary and Tertiary (EOR). While the primary recovery relies on the naturally occurring pressure within the oil bearing reservoir to push the oil to the surface. The drawback of this technique is that it leaves 85%-95% oil behind. Secondary oil recovery techniques involve water injection (water-flooding) or pumping compressed

gases into the reservoir. While this technique leaves about 50-80% oil in the reservoir. The tertiary techniques (EOR) can be grouped into [25, 31].

- Thermal EOR
- Gas EOR
- Chemical EOR
- Hydrodynamic EOR
- Combined EOR

Further research into developing EOR techniques is needed as the global demand for oil is increasing and more viable extraction solutions are needed to increase oil recovery.

This experiment investigates the behavior of ferrofluid and the displacement of ferrofluids in a porous media under a magnetic effect. This limits length scales for this experiment with increasing distance. The magnetic field intensity decays with the inverse of the square root of distance. However, this has not affected the final configuration of ferrofluid in the fluid saturated medium. The predicted configuration is independent of the flow pathway and the heterogeneities involved with the porous media. The visual and post processed results have shown that the ferrofluids are capable of displacing a highly viscosity fluid (oil) and stabilizing the interface between the two fluids in the vicinity of a magnet.

1.2 Fluid Flow in Porous Media

Drainage is referred to as the displacement of a wetting fluid by the injection of a non-wetting fluid. The percolation of fluid through a porous media can evolve forming different flow patterns based on injection conditions and fluid- media properties [16]. Drainage in a fluid flow gives rise to three types of fluid regimes. Capillary fingering occurs during the injection of fluid which is more viscous than the fluid being displaced and this happens at slow injection rates. This further gives rise to irregular conduits or fingers called capillary fingering. When the flow rate is relatively higher, the fluid pervades uniformly through the media giving rise to a stable displacement. When the viscous forces govern the flow, the viscosity of the injected fluid is lower than the displacing fluid. This marks the onset and evolution of instabilities linked to viscosity variations called viscous fingering [16, 18]. The understanding of origin of flow instabilities can help form appropriate strategies for oil production in enhanced oil recovery, CO₂ migration in porous media, drug delivery, water transport in soil etc.

Immiscible displacement in porous media has been a topic of theoretical and experimental research for a long time. Several drainage experiments have been conducted with different porous media of multiple pore size distribution, specifically to observe the behavior of immiscible liquid blobs [12, 5]. The network approach used to represent porous media with a network of capillary tubes is a well-known technique that represents ideal approximation of percolation in porous medium. The fluid-fluid interface or fluid-gas displacements create flow pathways along one of the fluid flows forming patterns, one of the flows that forms patterns varying from compact to ramified to fingers [2]. Thus the understanding of this mechanism is important as it causes instabilities in fluid drainage system. This work focuses on two primary factors, viscosity and flow rates. While it has been achieved that drainage in a porous medium can be distinguished by two non-dimensional numbers, namely the capillary number (Ca) and the viscosity ratio (M)[17]. Capillary number is a non-dimensional number that describes the importance of viscous forces to capillary forces. Viscosity ratio (M) is the ratio between the viscosity of working fluid and the fluid in medium.

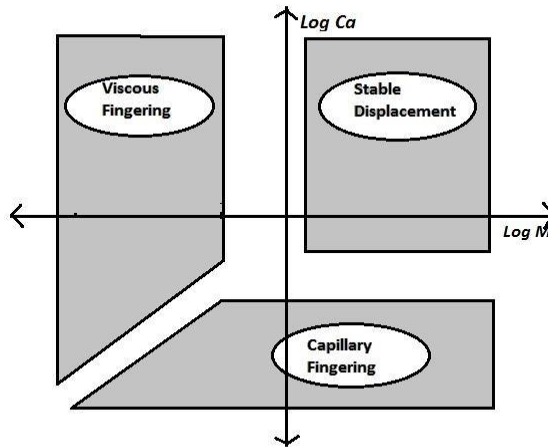


Figure 1.1: Drainage Phase Diagram

The type of percolation in a porous medium, whether it is drainage or imbibition.

Capillary forces play a pivotal role in porous medium, because the capillary forces act at the interface between the fluids which consists of many menisci that is at the pore scale and therefore are significant with respect to gravity and viscous forces. Water transport in the pore space can be explained by two fundamental concepts namely Wettability and Capillarity. When there are two fluids present in a pore space, one of them gets attracted by the wetting fluid, which is also called as wetting phase, while the other fluid is known as non-wetting[4]. Here the synonym used for water is wetting phase and non-wetting phase used for air. The thin films covering the surface will always have water present in small amounts. Hence water can be adsorbed from the vapor present in the pore air. Taking into account that a pore space looks like a collection of channels through which any fluid can flow. The effective width of which varies with length. The thickness of the layers depends on the strength of molecule- molecule interactions between the interface and water and on the relative air humidity. The tight bonding of the water adsorbed onto the surface makes it immobile. With the increasing levels of water in a porous medium, it gets attracted to the water adsorbed at the surface due to cohesion forces, and on the contrary tends to reduce the area of water air interface. This state of water occurs in small corners and is generally referred to as capillary water. Water collected near the edges of the pores is considered as pendular rings which is generally immobile and doesn't form

continuous flow paths. The pressure drops near the pendular regions and pore air. Adding more water makes the pendular water regions to fuse with one another and make continuous thicker films along the pore walls. At this stage the air occupies the central part of the pores continuously. As the water further increases the pores get entirely filled by water, the water film thickens up and the cross section gets smaller resulting in complete dissolution of air into water.

The experiment by Saffman and Taylor[22] for the displacement of one fluid by another one in a Hele-Shaw cell has shown how important the viscous forces are in stabilizing and destabilizing the interface depending on the viscosity of displacement fluid Taylor & Homsy, 2002[10]. Destabilization in return leads to fingering of the fluid. Thus the kind of displacement observed during drainage depends on the relative magnitude of viscous forces and capillary forces. In the absence of gravity, different flow regimes are expected depending on the capillary number. For displacements at low flowrates, the drainage is depends on the heterogeneity of capillary pressure which is well explained by invasion percolation theory [26, 19]. The capillary forces prevent the spontaneous entrance of a non-wetting fluid into the porous medium. When the difference between the wetting and the non-wetting fluid pressure is higher than CP, the non-wetting fluid will only enter a throat with radius R. Capillary pressure for which is given by $C P = 2\sigma_{nw} / R$, where σ_{nw} is the interfacial tension between the non-wetting(subscript n) and the wetting fluid (subscript w). This condition results in uniform pressure distributions between the fluids which is controlled by pore size distribution. This results in advancement of the displacement front. The fluid penetrates the largest pore throat which gives the smallest capillary resistance. When viscous forces become prevalent, the pressure distributions in both the fluids become non-uniform and the non-wetting fluid starts to invade the smaller throats because of the pressure difference. This invasion-percolation model has been successfully described in Lenormand et al [12] observed in their large number of displacement experiments for different fluid pairs that at different viscosity ratios and capillary numbers different flow regimes evolve. Viscosity ratio (denoted as M), is a measure of resistance to slow deformation by shear stress, which arises from collision between different fluid particles moving at different velocities. Capillary numbers can be defined as the relative effect caused by viscous forces vs surface tension between two immiscible fluids. When $M > 1$ at low capillary numbers, the displacement regime created capillary fingering. The displacement would slowly become stable at larger capillary numbers. But for low capillary numbers and with $M < 1$, capillary fingers were still observed[28]. However at higher capillary numbers and with the lower viscosity of invading fluids, viscous fingering dominated the drainage regime. Pattern identification and characterization of percolation is important for control & operation in many technologies. Of particular interest for this work, is

identification of pattern during percolation in a porous media and further stabilization of unstable drainage pattern with the use of ferrofluids and a magnetic field.

A good amount of research has gone into suppressing the conditions for fingering. For instance, Alkaline-surfactant-polymer (ASP) which is the secondary recovery mechanism has reduced the interfacial tension and the motion between the water and oil phase by reducing the residual saturation [27]. However, the use of alkali has introduced multiple problems for injecting the ASP solution. Deposition of alkali scales in the reservoir, and difficulty in treating the produced water are a few of the common issues observed with the use of ASP. This study aims at producing results from a promising technique that can suppress the formation of fingers by using a combination of ferrofluids and a proper oriented magnetic field.

The potential of controlling fluid movement to stabilize the drainage in a porous media with the use of ferrofluids is enticing. In this study a laboratory scale experimental setup was used to observe the behavior of ferrofluids in a porous media under a magnetic effect. The particles are of order 100 Angstroms (10 nm) in diameter and commonly magnetite, with the carrier liquid being either oil or water based. The flow of ferrofluid occurs at very low speed and Lorentz forces can be neglected. Ferrofluid was developed in the 1960s, with suspensions exhibiting strong magnetic behavior without losing its fluid characteristics under the influence of a strong magnetic field [30]. The immense behavior of ferrofluids have found potential applications in the field of microfluidic devices. When a ferromagnetic material is exposed to a magnetic field, the magnetic dipoles of the material aligns their dipole moment in the direction of magnetic field[20]. The particles stay suspended due to the thermal agitation caused in Brownian motion, while the surfactant coating inhibits aggregation or clustering of nanoparticles. Due to the small size of particles, ferrofluids can easily flow through porous media. The magnetic forces generated between the magnet and the ferrofluid enables it to flow in any desired direction through the control of a magnet in place[15]. Significant applications of this could be controlling placement of liquids, locating geophysically imageable liquids or treating chemicals.

The objective of this work is to inject two different ferrofluid (water-based and Oil-based) into two different porous mediums to control the flow under a magnetic field in order to control the instabilities caused by varying viscosities and flow rates. In this study, EFH1 (Oil based) and a water based ferrofluid has been used in the porous media. The experiment has been broken into three parts, first being the injection of ferrofluid into a porous media saturated with air and the second one with a porous media with oil. And the third being Injection of water (colored with food dye to give better visual access) to the oil saturated porous medium. The recent

improvements in the comprehensive image analysis techniques allow the determination of various fluid saturations in displacement experiments [28]. This research not only complements with the work of Lenormand & Zhang [28, 12] experiments, but also entails a study on suppressing the effects of fingering using ferrofluids. The results of this experiment show the viability of suppressing the drainage instabilities with the use of ferrofluids and a proper oriented magnetic field.

1.3 Objectives

- Demonstrate the suppression of instabilities in drainage when at least one of the working fluid is a ferrofluid in the presence of a properly aligned magnetic field.
- Observation of the drainage pattern of water in air saturated porous medium at different flow rates.
- Observation of the drainage pattern in an air saturated porous medium when a ferrofluid is injected at different speeds.
- Displacement of a higher viscosity fluid by a lower one (ferrofluids), in vicinity of a magnetic field.
- Observation of drainage pattern when water is injected into an oil saturated medium.
- Ferrofluid injection in an oil saturated porous media at different speeds.

These objectives are described in detail in the following chapters. Chapter 2 theoretically describes the analytical model used to define flow of nanoparticles in the presence of a magnetic field. Chapter 2 details the experimental methodology and the materials used in this effort. Chapter 3 defines the image analysis algorithms and discussion. All conclusions and future prospects of this thesis are defined in Chapter 3.

1.4 Analytical Model of varying magnetic field with distance

Two- phase immiscible flow has been rigorously studied for a porous medium due to its applications in oil recovery, hydrology and chemical engineering. When one fluid is displaced by the other and the displaced fluid in this case is wetting, it's called as Drainage, and when a non-wetting fluid is displaced by a wetting fluid it's called as imbibition (Zhou, 1992) [28, 29]. In a porous media the resulting displacement creates instabilities such as fingering patterns which

depend on the relative viscosity, speed of displacement, wetting properties, density, surface tension and length scales. The moving contact line has posed to be a problem in the finger formations, which can be defined as the fluid-fluid interface relative to the solid wall (Ashu et al 2008)[23]. During the displacement of an immiscible fluid by another fluid, the contact line 'slips' relative to the solid wall, which is in contrast to the no-slip boundary condition for a fluid-solid interface [3]. The approach for such a situation is dependent on the wetting properties of the fluids. When one fluid completely wets the surface or in other words when the contact angle between the wall and the fluid-fluid interface is small, the precursor film precedes the contact line. Thus slipping phenomena makes immiscible fluid displacement behavior dependent on the microscopic physical parameters governing the region around the contact line (Siddique et al, 2009)[24]. Effect of the gravitational force is negligible in drainage or imbibition. This can be demonstrated by bond number which is represented by equation 1.1. Since a magnetic field has been implied around the porous media, magnetic bond number plays a vital role. Magnetic bond number can be represented as

$$Bo_m = \mu_0 H^2 Z / \sigma \quad \text{_____} \quad (1.1)$$

Where Bo_m represents Magnetic Bond Number, H is the magnetic field strength, Z being the distance and μ_0 is the magnetic constant and σ is the surface tension between fluids. The Bo_m depends not only on the magnetic bond intensity on the fluid-fluid surface tension. The surface tension used were for water (79dynes/cm), water based Ferro fluid (21.8dynes/cm), motor oil Sw30 (21dynes/cm), Ferro fluid oil base (21dynes/cm). The interfacial surface tension can be calculated using the geometric mean relationship. This equation predicts the intermolecular forces acting between the two fluids [6].

$$\sigma_{12} = \sigma_1 + \sigma_2 - 2\sqrt{\sigma_1 \sigma_2} \quad \text{_____} \quad (1.2)$$

The flow of ferrofluid in a porous media varies with the type of magnetic field applied. A steady magnetic field pulls the ferromagnetic particles aligned in the direction of the field applied. The holding forces generated by the magnetic field results in a predictable configuration of ferrofluid around the magnet kept in the vicinity (Lf, Lawrence et al, 1998) [15].

Washburn described the porous media as a collection of capillary tubes. Darcy's Law describes one dimensional flow in a porous media, while for the event of wet-out flow, the Darcy's Law reduces to Washburn relation that describes the square of the distance traveled by the invading front is proportional to the time, the proportionality of which depends on the surface tension between the interface, viscosity and the pore diameter. When a wetting fluid is injected the surface tension pulls the liquid further ahead and to counteract this force the viscosity force provides resistance, which is proportional to the fluid flow velocity that increases with increase in the column length. Thus when a steady and strong magnetic field is applied in the vicinity, the magnetic forces dominate the flow in a pipe, eliminating the resistance caused by viscosity variations. This further accelerates the flow in a porous media around the magnetic field (Guide et al., 2016) [7].

The particles of a ferrofluid get randomly aligned without any magnetic field in place. When there is no magnetization, there generally is no long range order being observed between particle and the carrier liquid. The particles get magnetized and align themselves in the direction of the magnetic field. The variation of magnetic field with distance is used to characterize the effect of increasing distance between the magnetic field and the point of injection from the center. The magnetic field, H exerted on the surface is calculated using the following equation, 2.2(Levy et al., 1993, 1995) [13, 14].

$$H_x(x,z) = M/2\pi[\arctan z/x - \arctan (z-h)/x - \arctan z/(6+d) + \arctan (z-h)/(x+d)] \quad (1.3)$$

Z for this equation is the height of the porous media, which is 1.8mm. The value of H needs to be calculated in the X, Z plane, with keeping in account the value for M (Saturation Magnetization). X in this experiment is the lateral distance between the magnet and porous media. The value of H is calculated at different positions of X. The variable d is 6.35mm.

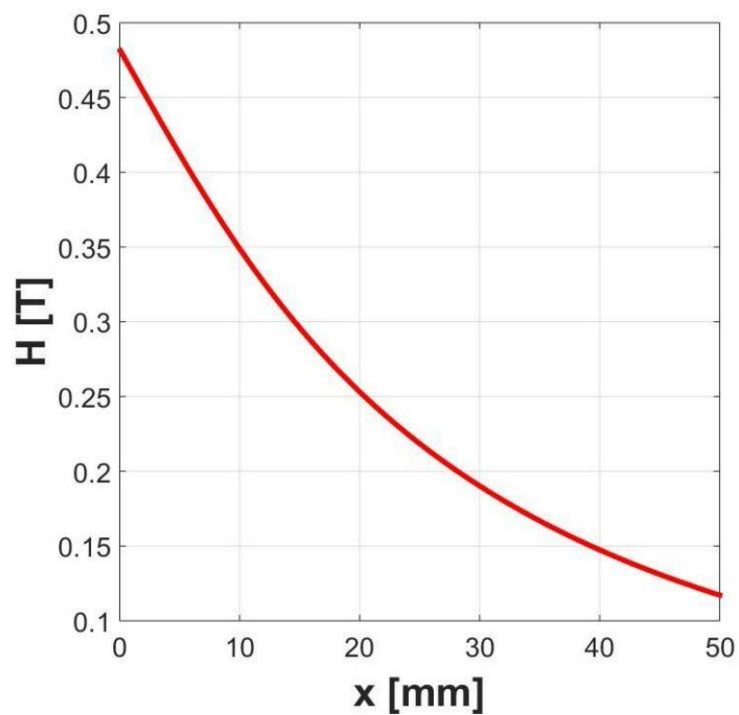


Figure 1.2: Magnetic field variation with distance

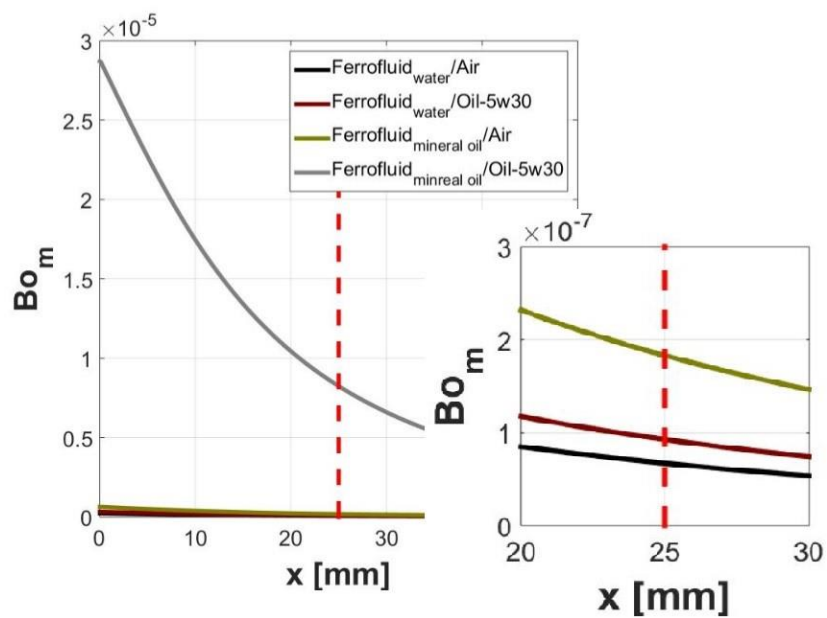


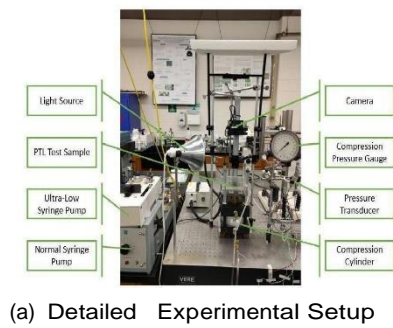
Figure 1.3: Magnetic Bond Number variation with distance

Chapter 2

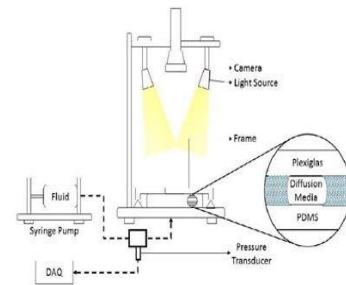
Methodology

2.1 Experimental Setup

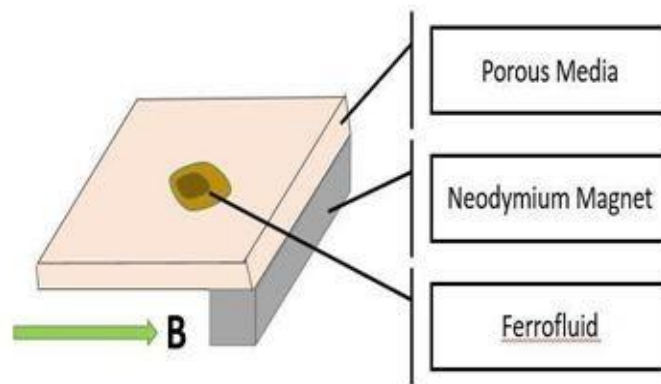
The porous media used for this study is a Styrofoam, which is made of Polystyrene. Polystyrene is an aromatic polymer made of styrene monomer. Styrofoam is a trade-marked name for Polystyrene which is used in household insulations, take-out food containers and appliance packaging. The porosity of the porous media varies from 30-40% depending on the conditions it's made under. The porosity for the Styrofoam used in the experiment is 40%. Styrofoam was cut into thin slices of 5.5 x 4.5 x 0.2cm, 5 x 5 x 0.18cm, 4 x 4 x 0.2cm, 5.5 x 4.2 x 0.2cm dimensions. The test samples were kept in the desiccator for 24 hours prior to every experiment (Medici, 2010) [18]. The latter was then placed between a PDMS (polydimethyl-siloxane) and a Plexiglas. PDMS is an optically clear, amenable and a hydrophobic material made of silicon known for its unusual flow properties used to seal the porous media while giving visual access. In order to avoid permeation between porous media and PDMS surfaces, the two layers were compressed with a Plexiglas. The entire cell was placed on a metallic frame which was kept in place with screws. Two different syringe pumps were used for the experiment. An ultra-low flow rate pump, Harvard Apparatus model 2274, was used for observing capillary fingering regime during the experiments, while for viscous fingering Harvard Apparatus model 938 syringe pump was used. The flow rate was varied to observe different flow regimes. Flow rate used for the experiments were 126 microlitres/min, 23.4 microlitres/min, 6.10 microlitres/min and 1.59microlitres/min. These flow rates were pumped through an ultralow syringe pump.



(a) Detailed Experimental Setup



(b) Configuration of working model of the setup



(c) Placement of magnet on the setup from the point of injection of fluids

Figure 2.1: Experimental Setup

A compression pressure gauge was used to compress the entire cell closer to the camera in place. A compression pressure of 2.5 psi was used for ferrofluid injection into air saturated medium and 2.0 psi for ferrofluid injection into an oil saturated medium. A CCD camera mounted 0.6 m from the top of the cell with an external light source was used to gather images of the drainage during the experiment. The PDMS layer with a 2mm diameter hole in the middle was used for injecting the working fluid using a 10 ml syringe pump, keeping the flow rate constant. Three different working fluids were used for the experiment. Initial results were observed by injecting water into air, and the second part of the experiment involved the use of EFH1 ferrofluids into the porous media saturated with air. The third part of experiment was conducted with the same ferrofluid as the working fluid and injected into the oil saturated porous media. All the experiments for this study were conducted at room temperature.

The top view images of the percolation experiment were captured using a CCD camera, which were further recorded using EPIX PIXCI imaging board and XCAP frame grabber. These images were then used to calculate the total area covered by the injecting fluid on the porous medium for each test. The time vs occupied area curve was referred to as the saturation curve (Medici, 2010) [18]. To obtain the exact displacement pattern, post image processing analysis were then carried out.

2.2 Experiment testing

2.2.1 Materials and Methods

This section describes the different materials used in the experiments which includes the fluids used such as ferrofluid- Mineral Oil based and water based, water, oil and the magnets used.

Ferrofluid-EFH1

The working fluid used is a mineral oil based ferrofluid (EFH1) which was used as received. Table 2.1 consists of the physical properties of the fluid used.

Table 2.1: Ferrofluid EFH1

Appearance	Black brown fluid
Carrier Liquid	Light mineral oil
Saturation Magnetization	440Gauss (44mT)
Viscosity at 27 ⁰ C	6cp (6mPa/s)
Particle Diameter	10nm
Initial magnetic susceptibility	2.58G/Oe (0.17emu/g/Oe)
Relative magnetic permeability at 20Oe	2.6
Density	1.21g/mL
Magnetic particle concentration	7.9%/vol
Flash point	92 ⁰ C
Pour point	92 ⁰ C
Surface tension	29dynes/cm (29 mN/m)
Volatility (1hour at 50 ⁰ C)	9%

Ferrofluid- EMG 308

The second working fluid used is a water based ferrofluid (EMG-308). Table 2.2 states the properties of this ferrofluid.

Table 2.2: Ferrofluid EMG 308

Appearance	Black brown fluid
Carrier Liquid	Water
Saturation Magnetization	66 Gauss (6.6mT)
Viscosity at 27 ⁰ C	5cp (5mPa/s)
Particle Diameter	10nm
Density	1.05-1.07 g/cc
Water Solubility	Complete
pH	7 - 9
Boiling Point	100 ⁰ C
Vapor Pressure (mm/Hg @ 20 ⁰ C)	17

Magnet- Neodymium (N45)

Neodymium magnets are the most widely used magnet type. It's a permanent rare earth magnet made from an alloy of iron, boron and neodymium to form the tetragonal crystalline structure represented as ND₂ Fe₁₄ B.

Table 2.3: Specification of Neodymium magnet - N45

Type	Rectangular block
Dimensions	3 x 0.5 x 0.25 inches
Tolerance	All dimensions \pm 0.004in
Material	NdFeB, grade N45
Plating	NiCuNi Triple layer coated
Maximum Op Temp	176 ^o F (80 ^o C)
Br max	13500G
Holding Power	33lb
Magnetized axis	Magnetized through thickness
Weight	1.8oz

Motor oil- Sw-33

Valvoline ILSAC Grade oil are fully synthetic premium oil designed to give high levels of fuel efficiency and meet the performance requirements.

Table 2.4: Motor Oil S w -33

Viscosity at 100 ^o C	8.8cst
Specific gravity at 15.6 ^o C	0.844
Flash COC ^o C	220
Pour Point ^o C	-45
CCS cup	4600
MRV TP - 1cP	30000
NOACK	12 wt%
Sulfated ash	0.93
Zinc wt%	0.83
Phosphorus wt%	0.076
Sodium wt%	0.049
Calcium wt%	0.211

Water

Water was used as a working fluid, and a coloring agent, dye was used to give better visual access. Table 2.5 incorporates the properties of water.

Table 2.5: Water Properties

Appearance	Transparent
Density	1,000 kg/m ³
Viscosity @ 25 ^o C	1cP
Specific Weight @ 5 ^o C	9.807kN/m ³

2.2.2 Methods

This experiment involved performing three different sets of experiments which were designed to explore the possible flow regime. During capillary fingering, water was injected into the media saturated with air at low capillary number using ultralow syringe pump. During this air was displaced by water and patterns with protruding conduits were observed which are called as capillary fingers. In the stable displacement experiment air was displaced by water at a relatively higher flow rate. The second step in the experiment involved air displacement from the porous media with ferrofluids being the working fluid. EFH1 and EMG 308 Ferrofluids were used with the 10nm sized particles dispersed in the colloidal suspension. The specification of both has been mentioned in the tables above. An external magnetic field was applied during the experiment to observe the changes in the porous media upon the injection of working fluid. This experiment was conducted at varying flow rates. Two magnets were placed close to the cell, to observe the effect of an external magnetic field on the drainage regime in the porous media. For capillary fingering, ferrofluid was injected using an ultralow syringe pump and higher speeds were used to observe viscous fingering.

The experiment was then taken further with the use of Motor oil to observe the displacement effect in porous media along with the ferrofluids and water. This experiment was broken into two parts. The first part involved the use of one neodymium magnet kept in the vicinity and the other one with two magnets kept together to experience the effect of magnetic field. The second part involved the use of no magnet to observe the effect of no magnetic field on the ferrofluids & oil in the displacement regime. Food Dye was then added to water to give it visual access, which was further injected to an oil saturated medium.

2.2.3 Water injection into an air saturated medium

The first set of the experiment involved partially repeating the experiments described in (Medici, 2010) [18]. The list of the experiments involved performing two different sets of experiments which were designed to explore the possible flow regime. During capillary fingering, water was injected into the media saturated with air at low capillary number using ultralow syringe pump at speeds 1, 6, 10, 14 and N 14 which corresponds to flow rates of 126 microlitres/min, 23.4 microlitres/min, 16.10 microlitres/min, 1.59 microlitres/min and 78000 microlitres/min respectively. During this step the air was displaced by water and patterns with protruding conduits were observed which are called as capillary fingers. The second reiteration involved injecting fluid at higher flow rates from the normal syringe pump into the porous media.

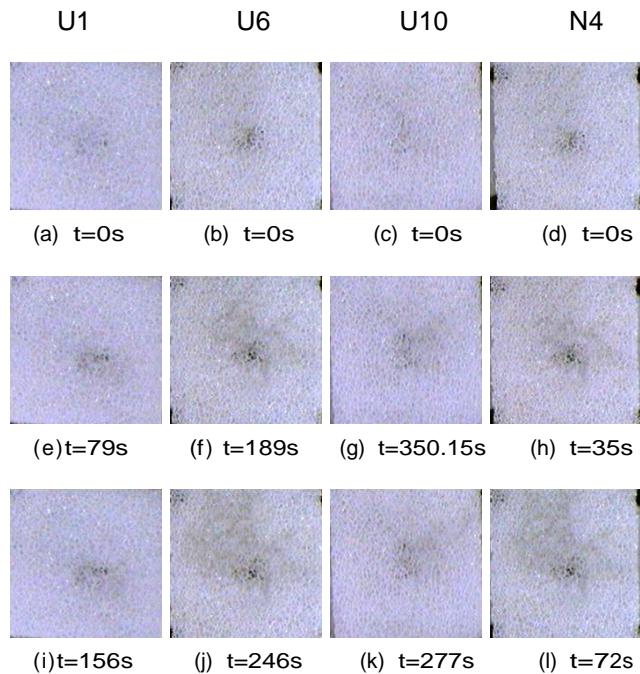


Figure 2.2: Water displacing air at pump speeds ultralow 1, 6, 10 and normal 4 respectively.

2.2.4 Water Injection into an Oil Saturated Medium

Water injection into an oil saturated porous media was taken out by adding a red color dye into water to provide visual access during the experiment. The injection was carried out at various flow rates to observe the fingering patterns.

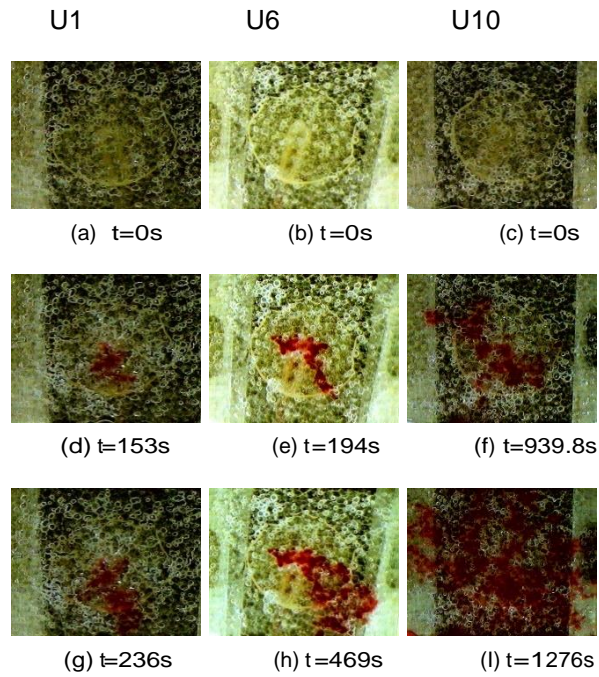


Figure 2.3: Water displacing oil at pump speeds ultralow 1, 6, 10

2.2.5 Oil Based Ferrofluid Injection into an Air Saturated Porous Media

Oil Based Ferrofluid Displacing Air with No Magnetic Field

This experiment involved displacing air from the porous media with ferrofluids as the working fluid. EFH1 and EMG 308 ferrofluids were used for this step. The description of the ferrofluids is given in table above. The working fluid was then injected from a 2mm diameter tube into the PDMS that contained the diffusion media kept under the Plexiglas compressed with the compression pressure of 2.5psi and 2psi. The flow rates used for this experiment were 126 microlitres/min, 23.4 microlitres/min, 16.10 microlitres/min and 1.59 microlitres/min.

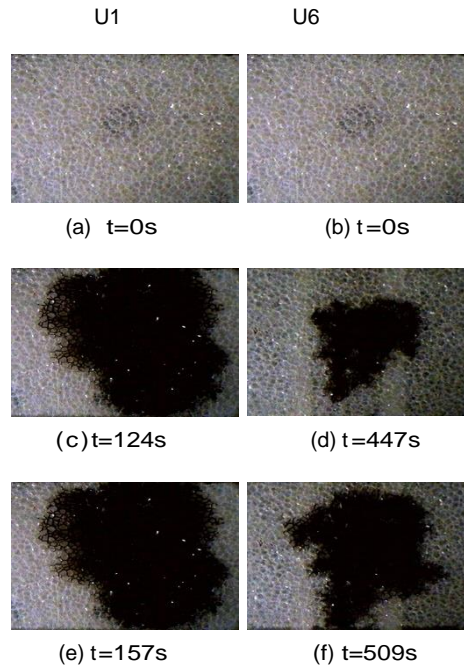


Figure 2.4: Oil Based Ferrofluid Displacing Air with No Magnetic Field at pump speeds ultralow 1, 6

Oil Based Ferrofluid Displacing Air in the Vicinity of a Magnet

This experiment involved placing a magnet close to the porous media (2.5cm from the center of the media to the magnet) to observe the effects of magnetic field on the ferrofluid and to investigate its effect on the configuration of the flow pattern. The magnet used for the experiment is a Neodymium magnet of grade N45. The magnet is magnetized through the thickness thus the N S poles are on the length (3inches) and breadth (1/2inches) respectively. The specifications of the magnet are given in Table 3. It was observed that the magnetic field was strong near the magnet rather than at the center of the porous media from where the injection took place as described in Chapter 2. The strong field caused the domains of nanoparticles to line up towards the magnetic field. Near to the magnet it was visually observed that the magnetic field had out pulled the gravity pull due to an accelerated motion around the magnet. This effect was observed at all flow rates, even though the results were more prominent at 126 microlitres/min, 23.4 microlitres/min, 16.10 microlitres/min and 1.59 microlitres/min.

2.2.6 Oil Based Ferrofluid Displacing Oil from an Oil Saturated Medium

The porous media was soaked into a Motor Oil to observe the displacement effect upon injection of ferrofluid into the media. This step was further broken into four parts. The first being, with injection of EFH1 in an oil saturated media, the second part involved the injection of EMG 308 in an oil porous media. Third and fourth parts were achieved by placing a magnet in the vicinity of the porous media.

Oil Based Ferrofluid Injection in the Vicinity of a Magnet

This step was executed by the use of one neodymium magnet kept parallel to the porous media to experience the effect of magnetic field on the ferrofluids. This involved immersing the porous media in oil under pressure prior to running the experiment. A petridish was used for the above, to immerse a 1.8mm thick, 2.2 *2.2inches long porous medium under pressure from a rectangular shaped Plexiglas. The porous media was allowed to sit in oil for approximately 15 minutes until all the pores were completely saturated with oil. Then EFH1 was injected from a 10ml syringe through an ultralow syringe pump at 126microlitres/min, 23.4microlitres/min, 16.10microlitres/min and 1.59microlitres/min speeds and the same steps were repeated for EMG 308 ferrofluid. The advantage of keeping the magnet parallel to the porous media was the ability to visualize the flow in porous media. It was observed that the fluid motion was accelerated towards the magnet and the nanoparticles were magnetized due to the field induced and aligned themselves in the direction of the magnetic field. The movement of the ferrofluid was recorded using various frame rates depending on the flow rate used. The video was snapped after 6 sec for 16.10 microliters/min flow rate using a time indexed CCD camera. The fluid in the porous media continued to migrate towards the magnet until it reached the edges and took the symmetric rectangular shape of the magnet in place.

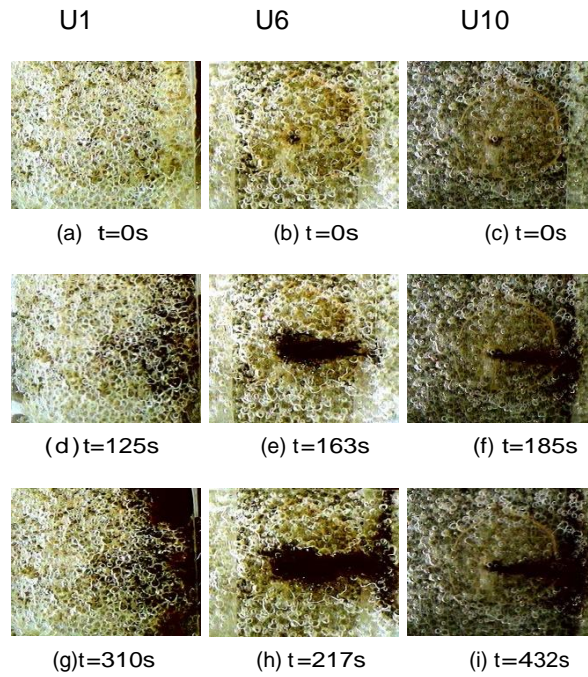


Figure 2.5: Oil Based Ferrofluid displacing oil in the vicinity of magnet at Pump speeds ultralow 1, 6, and 10

Oil Based Ferrofluid Injection without Magnetic Field

This experiment involved the use of no magnetic field to observe the displacement effect upon injection of ferrofluid in an oil saturated medium. The experiment was ran until the ferrofluids touched one of the edges and the flow was then eventually stopped. The configuration of ferrofluids in this case was observed to have protruding edges (finger like structures) spreading through the center of the porous media. The flow rates used for this were kept the same as for the experiment mentioned in previous section to maintain consistency in the results.

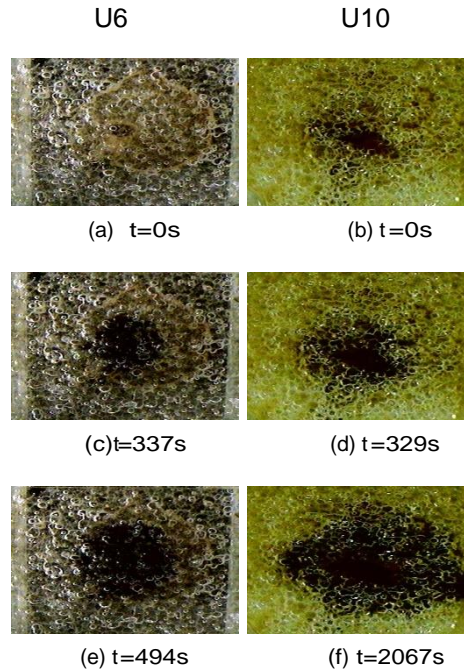


Figure 2.6: Oil Based Ferrofluid Displacing Oil with No Magnetic Field at Pump speeds ultralow 6, 10

2.2.7 Water Based Ferrofluid Injection into an Air Saturated Medium

Water Based Ferrofluid Displacing Air with No Magnetic Field

This experiment was conducted with EMG 308 as the working fluid and involved displacement of air from the porous media without any external force of magnetic field acting on it. The flow rates used for this set of experiment were in adherence with the oil based ferrofluid used, they were 126microlitres/min, 23.4 microlitres/min, 16.10 microlitres/min and 1.59 microlitres/min.

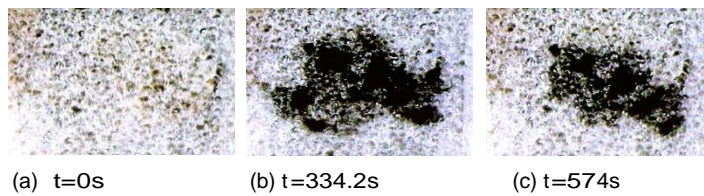


Figure 2.7: Water Based Ferrofluid Displacing Air with No Magnetic Field at pump speeds ultralow

Water Based Ferrofluid Displacing Air in the Vicinity of a Magnet

This experiment involved placing a magnet close to the porous media, at 2.5 cm distance from the point of injection of media to the magnet. It was done to observe the effects of magnet on the EMG 308 and to investigate the effect on the configuration of the flow pattern. The magnet used for the above is Neodymium magnet of grade N45. It was observed that the magnetic field was strong near the magnet and the accelerated movement of the ferrofluid was seen near the magnet. The ferrofluid seem to have aligned themselves around the magnet. It was visually observed that the magnetic field had out pulled the gravity pull due to an accelerated motion around the magnet. The effect was observed at all flow rates, even though the results were more prominent at 126 microlitres/min, 23.4 microlitres/min, 16.10 microlitres/min, and 1.59 microlitres/min.

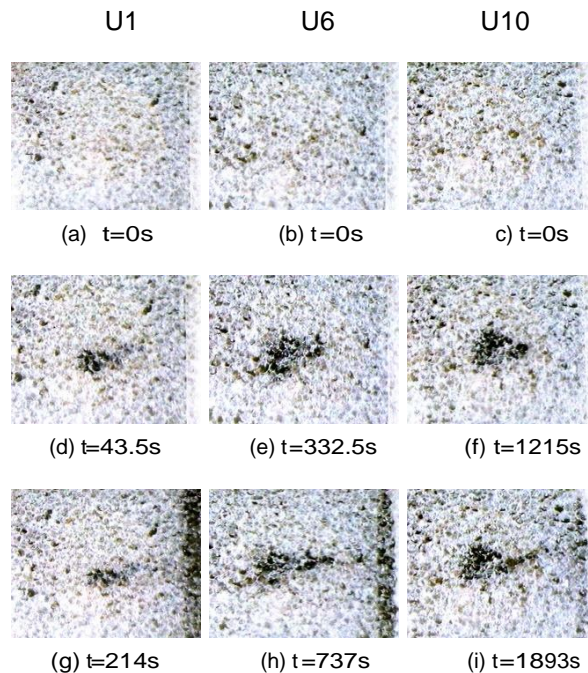


Figure 2.8: Water Based Ferrofluid displacing air in the vicinity of magnet at Pump speeds ultralow 1, 6, and 10

2.2.8. Water Based Ferrofluid Displacing Oil from an Oil Saturated Medium

The porous media for this experiment was soaked into a Motor Oil to observe the displacement effect upon injection of ferrofluids into the media.

Water based Ferrofluid Displacing Oil in the Vicinity of a Magnet

This step was executed by placing a neodymium magnet in the vicinity, at the same distance as it was done for EFH1 ferrofluid. The porous media was immersed in oil prior to the experiment. The magnet was then kept parallel to the porous media to get visual access of flow pattern during the experiment. It was observed that fluid motion was accelerated towards the magnet and the nanoparticles were magnetized due to the field induced and aligned themselves in the direction of magnetic field. Water based ferrofluid showed a pulsating flow motion towards the magnetic field. The images were captured at the speeds mentioned above. The frame speeds were set for different experiment based on the flow rates used. The video was snapped after 6 secs for 16.10 microlitres/min using time indexed CCD camera.

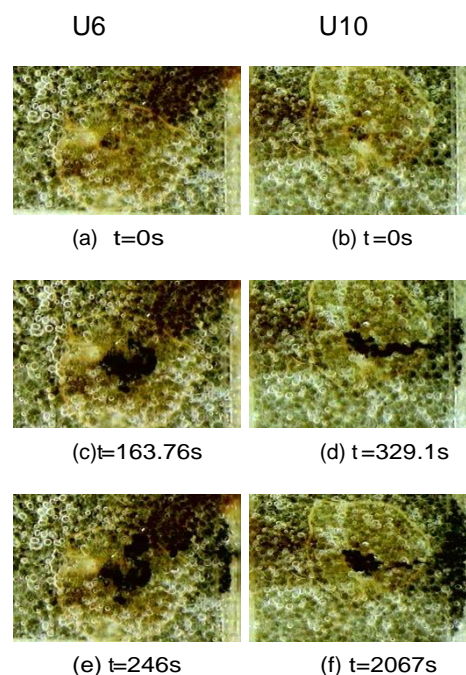


Figure 2.9: Water Based Ferrofluid displacing oil with Magnetic Field at Pump speeds ultralow 6, 10

Oil Based Ferrofluid Injection without a Magnetic Field

This experiment was conducted without the use of a magnetic field in the vicinity. The flow rates used were kept consistent for this experiment. The experiment was ran until the ferrofluids touched one of the edges of the experiment. It was observed that the ferrofluid in this case had protruding (finger like structures) edges spreading throughout the center of the porous media.

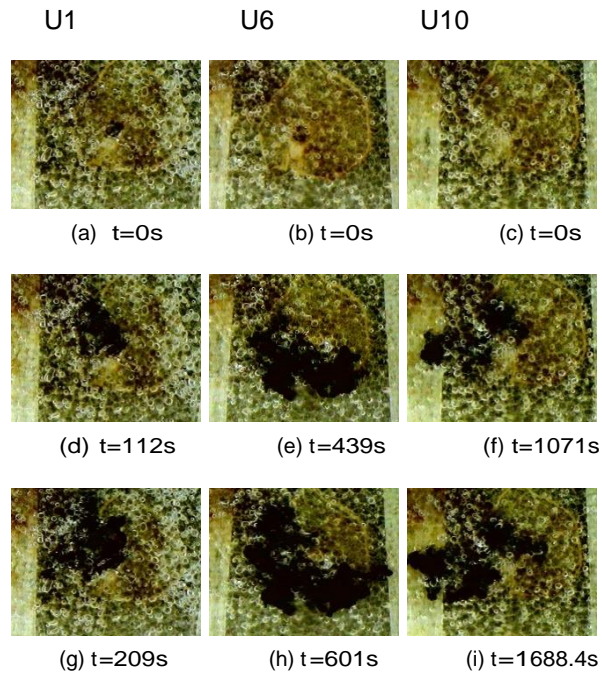


Figure 2.10: Water Based Ferrofluid displacing oil at pump speeds ultralow 1, 6, 10

2.2.9 Table for Experiments Conducted

Table 2.6: List of Experiments

Medium	Medium	Type of	Magnetic	Magnet position	Type of Magnet
Water	Air	Ultralow speed-	NO	-	NONE
Water	Oil	Ultralow speed-	NO	-	NONE
Ferrofluid(EFF	Air	Ultralow speed positioned at	NO	-	NONE
Ferrofluid(EFF	Air	Ultralow speed positioned at	YES	Right of the porous media- 2.5 cm from the	Neodymium
Ferrofluid(EFF	Oil	Ultralow speed positioned	NO	-	NONE
Ferrofluid(EFF	Oil	Ultralow 1,6,10	YES	Right of the porous media- 2.5 cm from the	Neodymium
Ferrofluid	Air	Ultralow pump positioned at 1,	NO	-	-
Ferrofluid	Air	Ultralow pump positioned at 1,	YES	Right of the porous media- 2.5 cm from the	Neodymium
Ferrofluid	Oil	Ultralow pump positioned at 1,	NO	-	-
Ferrofluid	Oil	Ultralow pump positioned at 1,	YES	Right of the porous media- 2.5 cm from the	Neodymium

Note: U1, U6, U10, U14 & N4 correspond to flow rates of 126 microlitres/min, 23.4 microlitres/min, 16.10 microlitres/min, 1.59 microlitres/min and 78000 microlitres/min respectively.

Chapter 3

Image Post Processing and Data Analysis

3.1 Image Post Processing

The process was initiated by transforming the grey scale images that were taken during the experiment. These images were collected to obtain the fluid- fluid interface. A background image taken before the percolation started was used as a reference image of a porous media which was further subtracted from each image. The changes between the actual and reference pictures due to the fluid invasion could be easily seen by applying a threshold value to their difference. MATLAB code was used for the post analysis of the data collected. The interface between the injected and displaced fluids was obtained using the edge detection algorithm by Ramanujan Approximation for Ellipse Shape in MATLAB. Ramanujan Approximation gives an elementary formula that can calculate the shape of an ellipse with an approximation formula that gives the least error even when the ellipticity (in this case the protruding fingers or the instabilities) increases. The reconstruction of the images was done by plotting the border points of the fluid interfaces captured at different time intervals.

The MATLAB code was written such that the area on the diffusion media saturated by the injected fluid is referred to as the wetted area, denoted by A . The front length which is also the interface length between the displaced and the injected fluid is referred to as S . Using the above technique, A and S were calculated at each time interval during all stages of experiment. The wetted area was calculated using the length and width of the test sample, L and H respectively. The length and Height in this case were 5.2cms x 5.2cms respectively.

Hence, the projected area would be $L \times H$ which was then non-dimensionalized by the front length which was the perimeter of the test sample denoted by $2(L + H)$ calculated using the edge detection algorithm. Experiment setup file was created to give inputs to the three MATLAB codes which were run for the image processing. The parameters used were:

- Speed of the camera, 'dt', the value was given in seconds when the camera generator was used else was given a 0 value for a signal generator.
- 'Syr' was used to define the syringe size used for the experiment, in this case a 10ml syringe setting was used.
- 'Pos' this depicts the position of the pump. The experiments were done at ultralow speeds, positioned at 1,6,10 and 14 which relates to 126 microlitres/min, 23.4microlitres/min, 16.10microlitres/min and 1.59microlitres/min speeds respectively. The other setting used was for the normal syringe pump was positioned at 2 and 4.
- 'Pump', this variable was used to define the pump type used for the experiment setting.
- 'EPIX PIXCI', the image acquisition software used a synchronized method, which allows the camera to output a frame immediately when it receives a trigger. The inbuilt unique clock system ensures precise synchronization of all images.

3.2 Observations

3.2.1 Water Displacing Air

During this experiment, water was injected into an air saturated porous media at a very small Ca. The quasi-steady capillary equilibrium was achieved by the working fluid due to the slow injection of flow rate. The injected fluid entered only through the pores that gave the least capillary resistance, thus being the largest pores or the ones with the least internal angle (Gurau et al., 2006)[9]. This type of fluid injection had an irregular shape contrary to the stable displacement regime. This type of pattern is characterized by the formation of fingers or irregular conduits through the porous media

called as capillary fingering. The pressure applied by the syringe pump is higher than the capillary pressure of the medium. This lets the displacement of water-air interface in the diffusion media. However, the displacement is interrupted due to the ultralow flow rates used, which ceases the water-air interface movement, because the volume of water in the syringe pump is not enough to keep the menisci moving forward.

With increase in Ca or the flow rate, the time required for the fluid to reach one of the edges is less. And at relatively higher values of Ca , the fluid reaches a region of stable displacement, and the pressure keeps increasing. This trend changes when the viscosities are altered. If the viscosity of the injected fluid is lower than the displaced fluid, the pressure keeps dropping until it reaches one of the corners.

The following figure shows water percolation at different times. These images were recorded at ultralow flow rate of U1 and U6. The borders of the image represents the percolation of fluid into the DM. The experiment was stopped when the water reached the edges of the sample. These figures comprehend to the interface lines between the injected and the displaced fluids. Figure 4.2, shows the wetted area by injected fluid over time. This was calculated by L and H of the porous media. The viscosity ratio for water-air interface used is 64.

The experiment ceased when the water reached the edges of the sample. The flow rates used for the experiments were 126 microlitres/min and 24 microlitres/min, respectively. In order to achieve these flow rates, an ultralow flow rate syringe pump was used, Harvard Apparatus model 2274. Different stages of the water percolation model are shown in 4.1. These figures comprehend to the interface lines between the injected and the displaced fluids.

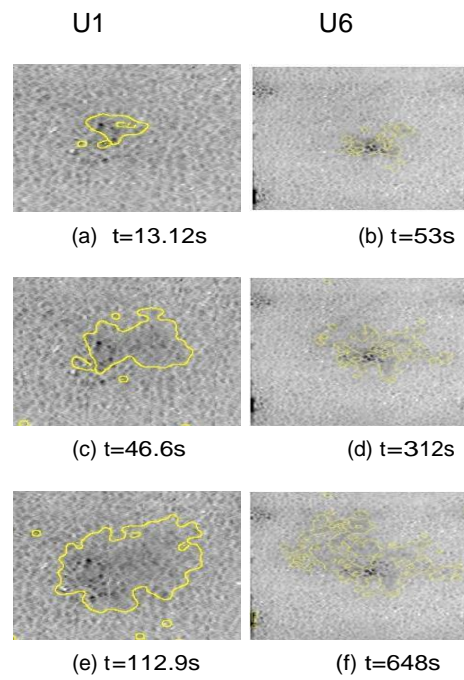


Figure 3.1: Water displacing air at the flowrates U1 and U6

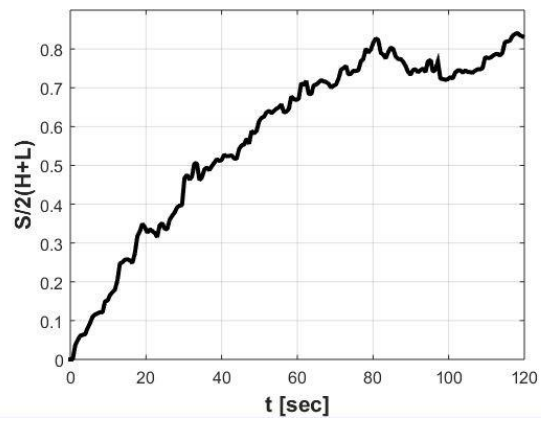


Figure 3.2: S Curve for water displacing air at flowrate U1

3.2.2 Water Displacing Oil

Food dye was added to water for this experiment to provide visual access when the latter was injected through an oil saturated medium. In an oil-wet medium when water was injected, a large amount of oil remained capillary trapped between the fingers. The water seemed to be in contact with the solid walls while the oil remained as a blob in the center which generated further instabilities like Food dye was added to water for this experiment to provide visual access when the latter was injected through an oil saturated medium. In an oil-wet medium when water was injected, a large amount of oil remained capillary trapped between the fingers. The water seemed to be in contact with the solid walls while the oil remained as a blob in the center which generated further instabilities like.

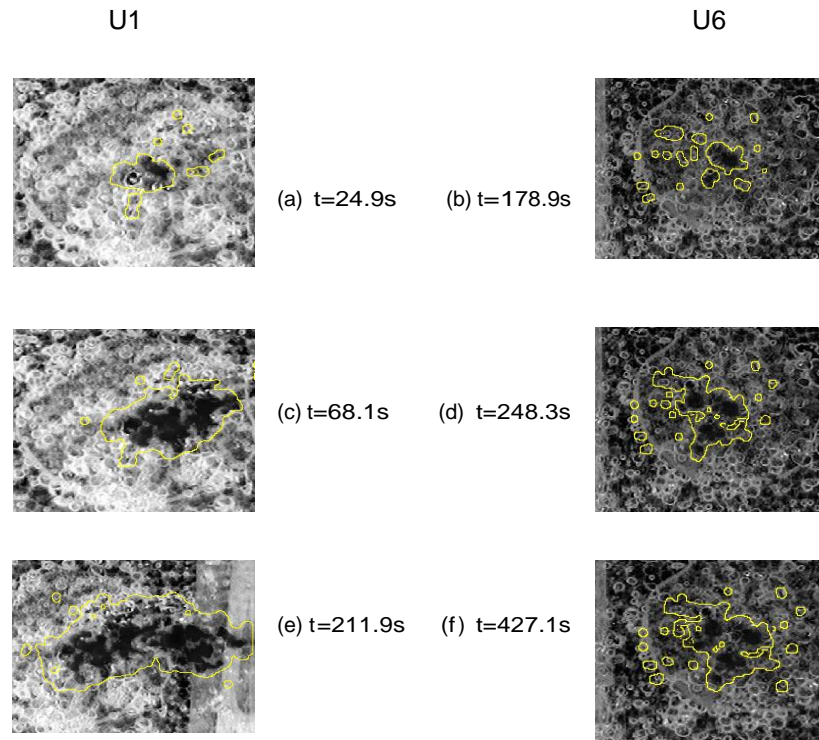


Figure 3.3: Water displacing oil at the flowrates U1 and U6

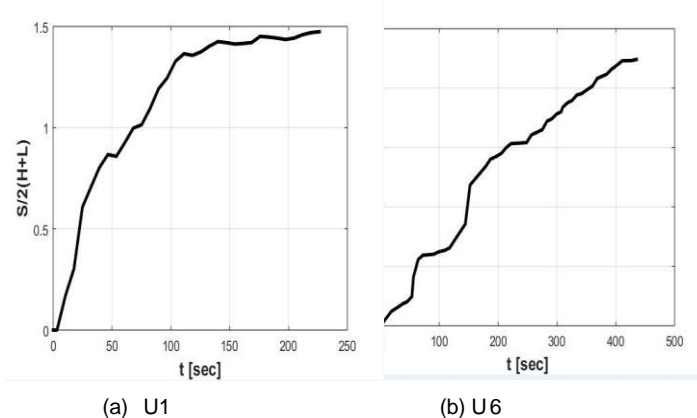


Figure 3.4: S Curve for water displacing oil at flowrate U1 and U6

3.2.3 Oil Based Ferrofluid in Air Saturated Medium

Oil based Ferrofluid Injection without magnetic field

These experiments involved injection of ferrofluid into the porous media. The ferrofluid used was EFH1 and the specifications for which have been mentioned in the table above. Injection of this working fluid was done at ultralow speed 126 μ liters/min, 23.4 μ litres/min, 16.10 μ litres/min and 1.59 μ litres/min speeds. After saturating the media with air, ferrofluids were injected to form an initial irregular shaped circle. It was observed that the nanoparticles of the ferrofluids were randomly oriented in the carrier liquid, and the flow was restricted because of the viscosity variations. The viscosity of the ferrofluid (6cp) is higher than air (0.00018cp) which shows strong resistance to flow and dissipates large amount of internal energy due to the friction in shear layers. (Franklin et al, 2003). Images for U1 were captured after an interval of 6 seconds.

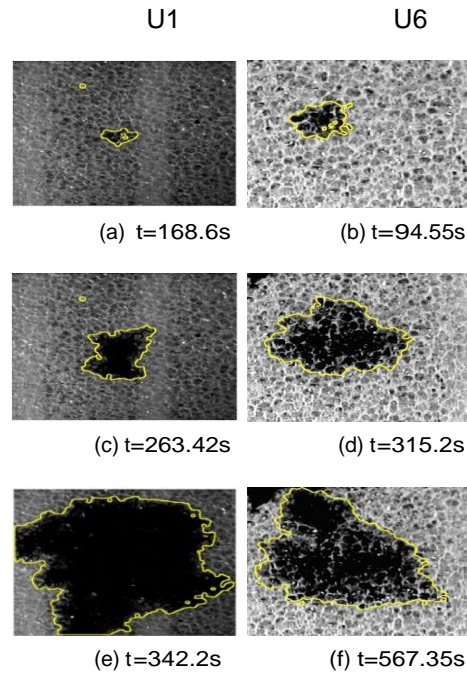


Figure 3.5: Oil based ferrofluid displacing air without a magnetic field at the flowrates U1 and U6

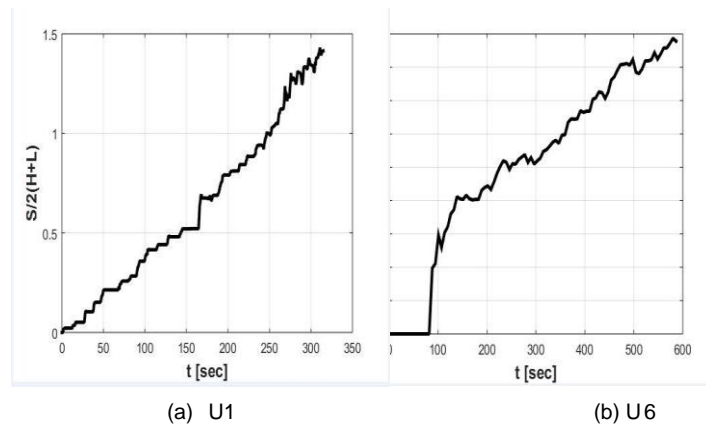


Figure 3.6: S Curve for Oil based ferrofluid displacing air without a magnetic field at U1 and U6

Oil Base Ferrofluid Injection into an Air Saturated Porous Media with Magnetic Field in Vicinity

The placement of a Neodymium magnet was done at stage three of the experiment. The magnet was placed parallel to the porous media on the setup tray and the Porous media on the PDMS was compressed at 2.5psi. Ferrofluid was injected through the 2mm thick tube to the PDMS. Ultralow flow rate of 126microlitres/min, 23.4microlitres/min, 16.10microlitres/min and [33]

1.59microlitres/min speeds, positioned at 1, 2, 6 and 10 were used to validate the results of ferrofluid injection with and without magnetic field in vicinity. It was observed that after few minutes of running the experiment, the magnetic field generated had aligned the nanoparticles which magnetized the ferrofluid, because of which the motion towards the magnet was observed. As the fluid approached the magnet the fluid motion became accelerated, because of greater magnetic strength near the magnet. After the fluid reached the closer to the edge of the magnet, it took the symmetric shape of the magnet. In this case the motion of ferrofluids wasn't affected by the viscosity difference. The motion of the fluid was completely magnetically controlled and it had out pulled the gravitational forces acting on the fluid. This takes us back to our objective that the motion of ferrofluids in the vicinity of a magnetic field is irrespective of the heterogeneities and the initial flow pathway. The predictive shape of the ferrofluids can find potential applications in many restoration activities that requires precise displacement of liquids.

3.2.4 Water Based Ferrofluid in an Air Saturated Medium

Water Base Ferrofluid Injection without a Magnetic Field

This experiment involved injection of water based ferrofluid(EMG308) into an air saturated porous medium. The images shown below are for injection flowrates 126microlitres/min and 23.4 microlitres/min. The observations were concluded to be the same as the oil based ferrofluid injection into an air medium. The nanoparticles of the ferrofluids were observed to have randomly oriented themselves to form an irregular shaped circle. The viscosity of the ferrofluid(5 CP) is higher than air(0.00018 CP) which reflects strong resistance to flow and dissipates large amount of internal energy due to the friction in shear layers.

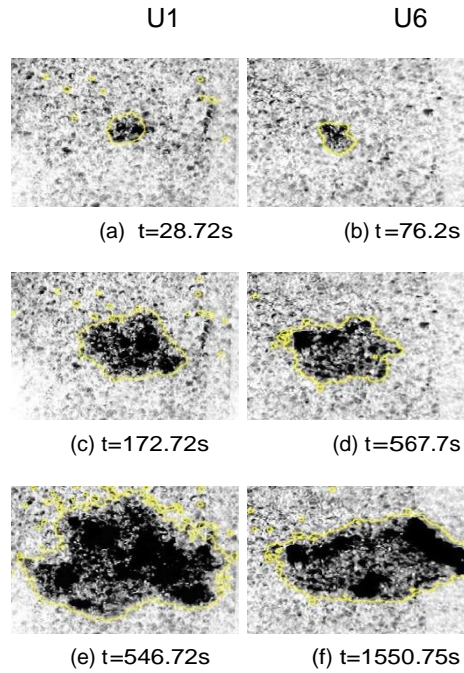


Figure 3.7: Water based ferrofluid displacing air without a magnetic field at the flowrates U1 and U6

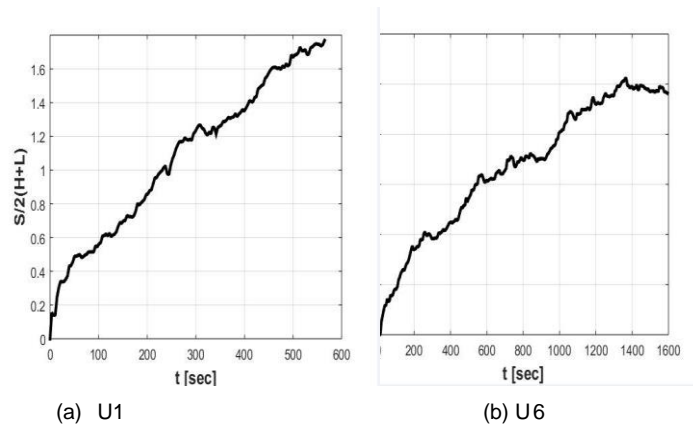


Figure 3.8: S Curve for Water based ferrofluid displacing air without a magnetic field at flowrates U1 and U6

Water Base Ferrofluid Injection with a Magnetic Field in vicinity

The neodymium magnet was placed parallel to a porous media on the setup. Ferrofluid was then injected through a 2mm thick tube. It was observed after a few minutes of running the experiment, the magnetic field generated had aligned the nanoparticles, which magnetize the ferrofluid, hence the accelerated motion of ferrofluid close to the magnet was seen. After the fluid reached closer to the edge of magnet, it took the symmetric shape of the magnet, thus inferring the viscosity variations and the surface tension didn't affect the motion of water based ferrofluid towards the magnet. The accelerated motion was solely because of the force of magnetic field on the fluid. This in turn proves the hypothesis that the potential application of the magnetic field can be used for controlling the interface of fluid interaction and the motion is irrespective of the heterogeneities.

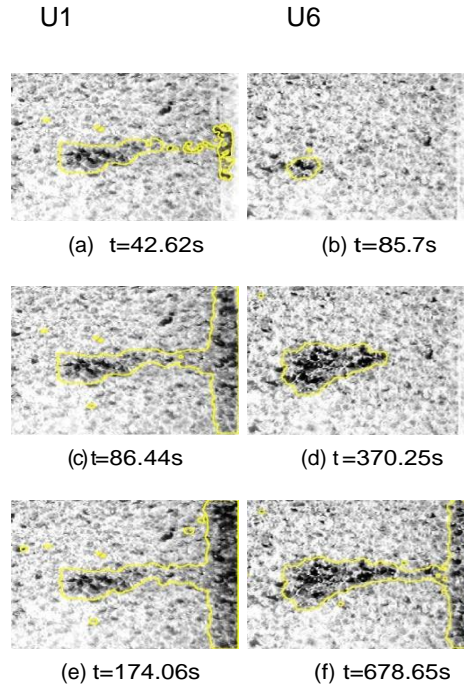


Figure 3.9: Water based ferrofluid displacing air with a magnetic field in vicinity at the flowrates U1 and U6

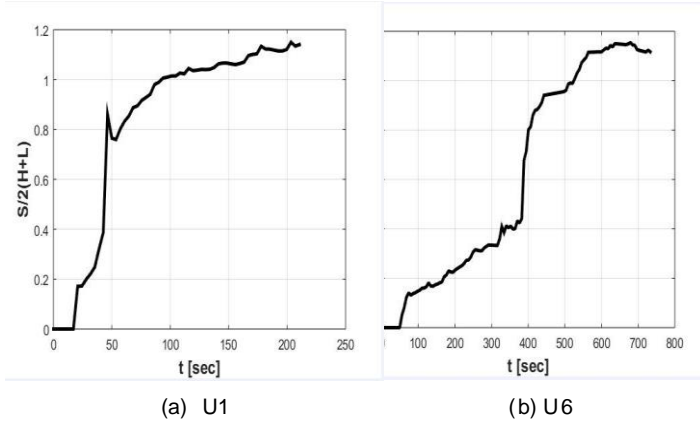


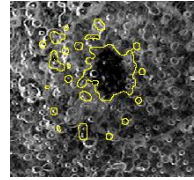
Figure 3.10: S Curve for Water based ferrofluid displacing air with a magnetic field in vicinity at flowrates U1 and U6

3.2.5 Oil Base Ferrofluid in an Oil Saturated Medium

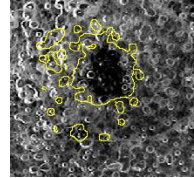
Oil Base Injection without a Magnetic Field

This experiment was conducted by using Motor Oil, Sw 30. Prior to performing the experiment with the ferrofluid, the porous media was immersed in oil under pressure from a Plexiglas until all the pores were soaked in oil. Ferrofluids were then injected from a 2mm tube into the PDMS tray containing the media immersed in oil. The post processing of these images showed drainage instabilities due to the viscosity variations, oil being more viscous than ferrofluids. This is observed due to the resistance provided by oil in pores due to its high viscosity. The fluid flowing near the wall of pores moved slower than the fluid in the center (oil being the one in the center). This resulted into the formation of capillary fingers, since low flow rates were used, namely, 126 microlitres/min, 23.4 microlitres/min, 16.10 microlitres/min and 1.59 microlitres/min respectively.

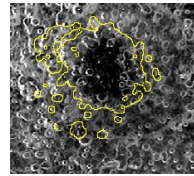
U6



(a) $t=181.2s$

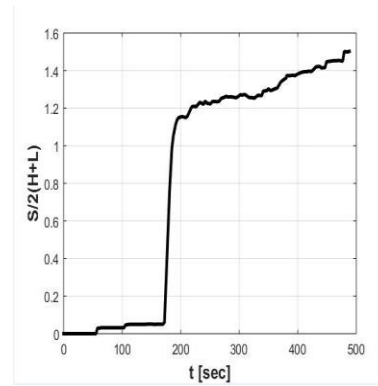


(b) $t=226.5s$



(c) $t=485.75s$

Figure 3.11: Oil based ferrofluid displacing oil without a magnetic field at the flowrates U1 and U6



(a) U6

Figure 3.12: S Curve for Oil based ferrofluid displacing oil without a magnetic field at flowrates U1 and U6

3.2.6 Oil Based Injection into a Ferrofluid with Magnetic Field in Vicinity

When a magnet was placed near the setup it was observed that the ferrofluids aligned their domains towards the magnetic field. The processed images infer that the ferrofluids started behaving as a homogenous single phase, with all the domains aligned towards one side under magnetic effect. This enables the ferrofluids to flow in a predictable fashion overcoming all the other governing forces like of gravitational and viscous. The motion of ferrofluid under a magnetic field is primarily due to the exerted magnetic field. (Borglin et al., 2000) This takes us to our objective that the lower viscosity fluid (ferrofluid) can displace the high viscosity fluid under a magnetic field had pushed the oil into the PDMS tray and started to accommodate themselves through the pores while displacing the oil. The accelerated movement of the ferrofluid towards the magnet was observed near the edges.

The accelerated motion observed in Figure 4.6 is due to the increase in magnetic strength around the magnet. Experiment was ran at varying ultralow speeds of 126microlitres/min, 23.4microlitres/min, 16.10microlitres/min and 1.59microlitres/min speeds, positioned at 1, 2, 6 and 10. Regardless of the ultralow speed, the end configuration of the fluid pushing oil from the pores and accumulating around the magnet was observed in every case. The images below demonstrate the motion of the working fluid at 16.10microlitres/min speed. After letting the porous media sit for an hour around the magnet the pattern was observed to be the same. Although it was hard to see the oil being displaced through eyes because of the light color of oil and the opacity of the ferrofluid. The fact that ferrofluid moved towards the magnet through an oil saturated medium shows the displacement of oil by ferrofluids in the vicinity of a magnetic field.

The placement of a Neodymium magnet was done at stage three of the experiment. The magnet was axially placed on the setup tray and the Porous media on the PDMS kept under 2.5 psi. Ferrofluid was injected through the 2mm thick tube to the PDMS. Ultralow flow rate of 1, 2, 6 and 10 were used to validate the results of ferrofluid injection with and without magnetic field in vicinity. It was observed that after 40 minutes of running the experiment, ferrofluid started accommodating itself through the pores towards the magnet and eventually took the shape of the magnet which was rectangular. Although the ferrofluid seemed to have flowed through the entire width of the darkened band, but the flow of ferrofluid near the vicinity of magnet was observed to have been greatly accelerated. The importance of using ferrofluids and magnets to achieve consistent and predictable shapes (like of a magnet) is crucial because many environmental restoration activities require precise displacement of liquids [11].

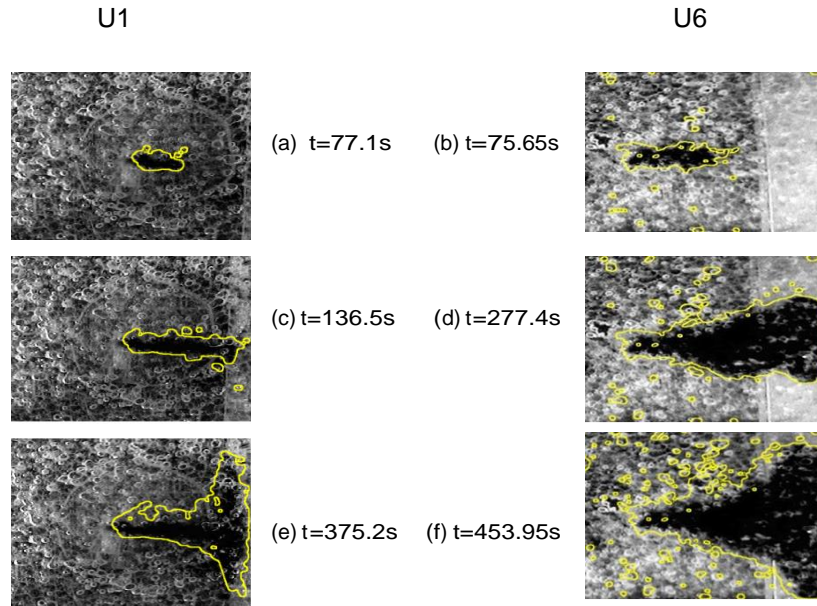


Figure 3.13: Oil based ferrofluid displacing oil with a magnetic field in vicinity at the flowrates U1 and U6

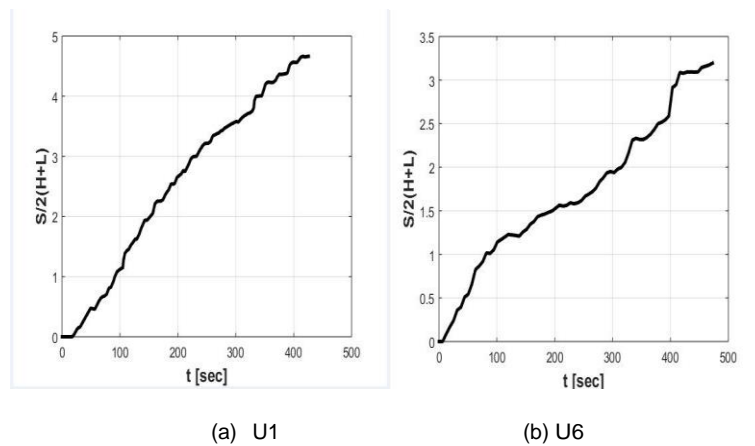


Figure 3.14: S Curve for Oil based ferrofluid displacing oil with a magnetic field in vicinity

3.2.7 Water Based Ferrofluid Injection in an Oil Saturated Medium

Water Based Ferrofluid Injection with No Magnetic Field

The processed images of these experiments ran at low flow rates showed similar drainage instabilities as observed with the oil based ferrofluid. The edge detection algorithm used to detect

the circumference of the displacement regime of ferrofluid in oil, depicted finger protruding. Due to viscosity difference, the shear resistance reduced the flow of ferrofluids in the medium.

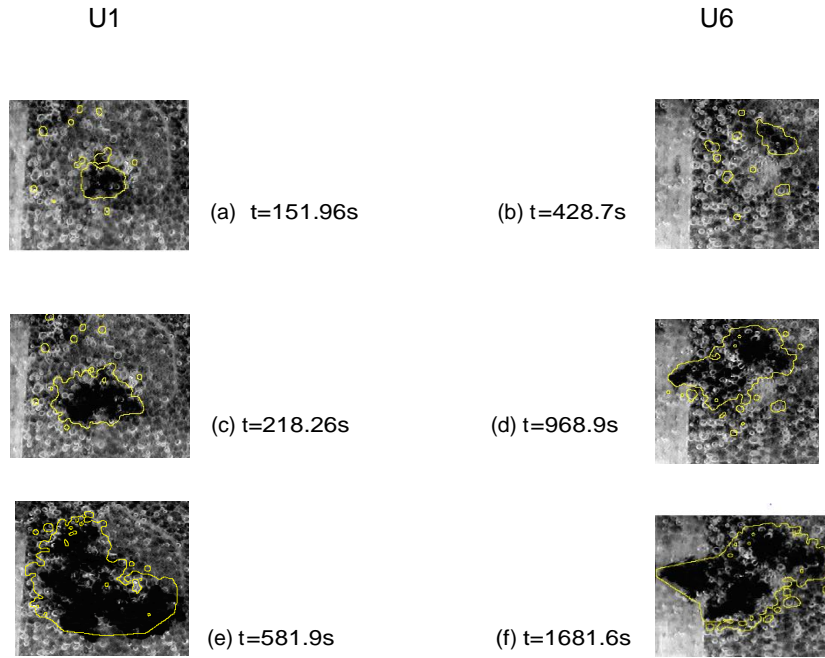


Figure 3.15: Water based ferrofluid displacing oil without a magnetic field at the flowrates U1 and U6

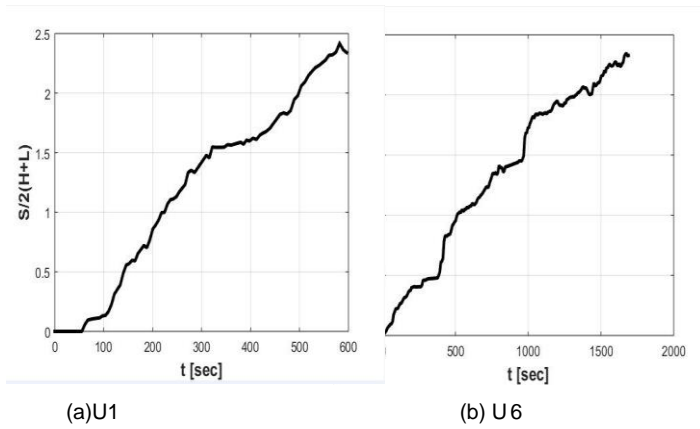


Figure 3.16: S Curve for Water based ferrofluid displacing oil without a magnetic field in vicinity at flowrates U1 and U6

Water Based Ferrofluid Injection with Magnetic Field in Vicinity

When a magnet was placed near the setup, the force due to an external magnetic field produced very strong forces on the ferrofluids that resulted in accelerated motion near the magnet. It was observed that with increasing distance between magnetic field and the ferrofluid, the forces had weakened which caused decrease in flow velocity of ferrofluid. When the ferrofluid approached the magnet, due to strong magnetic field the velocity increased. Regardless of initial configuration of ferrofluid, the final configuration is similar as to the oil based ferrofluid. Larger surface area requires more energy to stabilize, thus to minimize energy, fluids tend to take the shape with smallest surface area, hence the water based ferrofluids formed small drops during their motion towards the magnetic field. The final configuration was a pool near the magnet and there were limited retention effects observed at the advancing front.

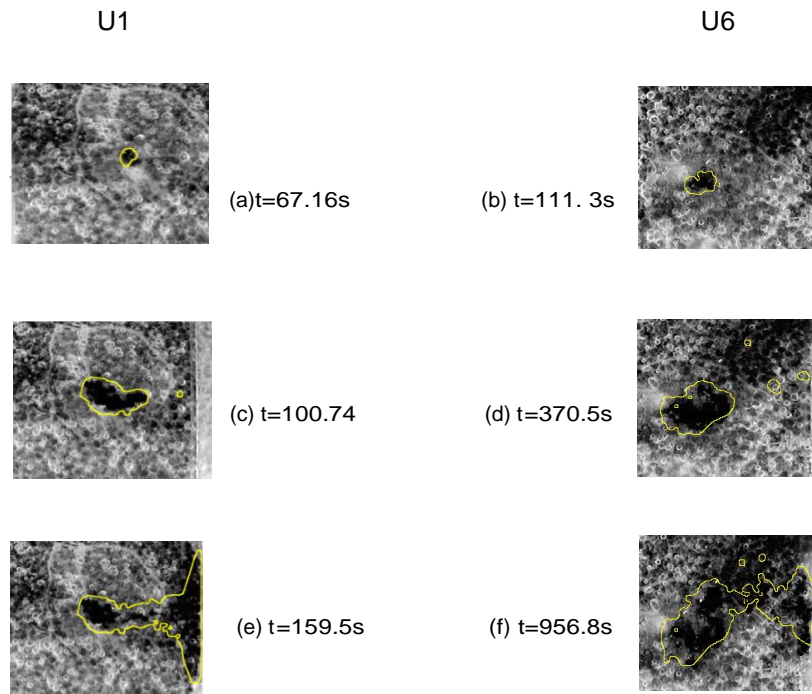


Figure 3.17: Water based ferrofluid displacing oil with a magnetic field at the flowrates U1 and U6

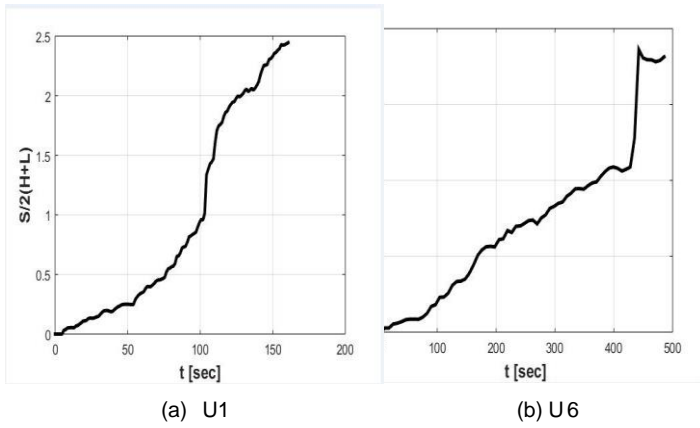


Figure 3.18: S Curve for Water based ferrofluid displacing oil with a magnetic field in vicinity at flowrates U1 and U6

Chapter 4

Summary and Conclusion

4.1 Summary

Different displacement experiments were conducted using different fluids, Ferrofluids namely, EMG 308 and EFH1, water, and oil. The porous media used was initially saturated with air and then oil. The working fluids were then injected through both the mediums at different times with different flow rates. The objectives of the experiments presented in this study were to demonstrate the suppression of drainage instabilities when at least one of the fluid is a ferrofluid working in the vicinity of a properly placed magnetic field. The initial experiments conducted with water as a working fluid being injected into an oil saturated medium, lead to capillary fingering at slow flow rates. When the same working fluid was injected through an oil saturated medium, multiple fingers which are characteristics of drainage instabilities were observed at the same flow rates used for water injection into air. Ferrofluids were further introduced to observe the displacement of a higher viscous fluid (oil) by a lower viscosity fluid such as ferrofluids. The random alignment of ferrofluids in an oil and air saturated medium was observed, which resulted in an irregular shape of ferrofluids in the medium. As mentioned in chapter 2, the viscosity of oil based ferrofluid is 6cp and water based ferrofluid is 5cp, for oil is 8.8cp and for air is 0.00018cp. Viscosity played a major role in the displacement of fluid through oil and air saturated mediums. The experiment was running at ultralow flowrates due to which there was low resistance in the shear layers of the porous media that resulted in dissipation of internal energy. Hence, to overcome these internal resistances, a magnetic field would provide amenable motion to the ferrofluid. It was observed that the force generated by the magnetic field, rivaled the internal resistance due to viscosity and capillary variation between the fluids. Further, after the ferrofluids got mobilized by the magnetic field, they took a steady and a predictable configuration around the magnet.

The water base ferrofluid was observed to have a pulsating flow around the magnetic field. It can be explained as the ferrofluid got closer to the magnet, the pulling magnetic force acting over the water base ferrofluid is stronger as shown in Chapter 2. Once the fluid reached closer to the magnet, it starts experiencing two opposite pulling forces (surface tension and viscous forces) parallel to the magnet. These two forces further result in an even string pulling force over the ferrofluid which resulted in a two cluster formation of ferrofluid. As the injection continued, the two clusters form again only to break when it gets closer to the magnetic field as the magnetic pull generated is greater than the parallel forces acting on ferrofluid. This later resulted in a pulsating flow. The final configuration was a pool of ferrofluid near the magnet with limited retention effects observed at the advancing front. The results observed in chapter 3 are in coherence with the objective stated which was to control the fluid/fluid interface and to stabilize the instabilities (fingers) observed during the displacement of a higher viscosity fluid by a low viscosity in the vicinity of a magnetic field. The motion in ferrofluid is mainly due to the alignment of nanoparticles with the field and the magnetization of ferrofluids caused by the field. Thus on exertion of magnetic force, the fluid acts like a single phase liquid ignoring the viscous and the gravitational forces. (Borglin et al., 2000). The fact that the viscosity of oil which is higher than ferrofluids didn't affect the motion of the ferrofluids towards the magnet. Instead the oil was displaced from the pores and was accumulated towards the magnet.

These observations have ramifications in engineering applications such as guiding to a target zone, displacement of viscous barriers like oil. These implications have an immediate application in enhancing oil recovery, imaging traces, locating cracks and fractures by injecting ferrofluid and detecting through surveys where the leakage takes place.

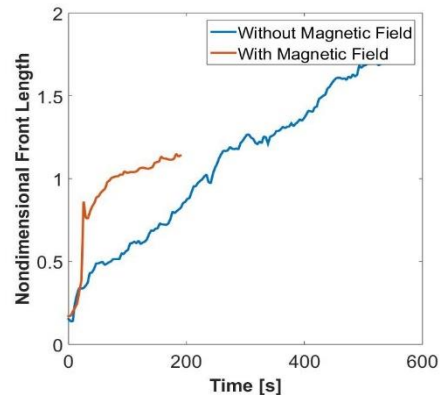
The limitation in this issue is the light color of the oil and opacity of ferrofluid which makes tracing the motion of oil in the petridish difficult. Estimation of the volume of oil during displacement could be the future study with respect to this research.

4.2 Conclusion

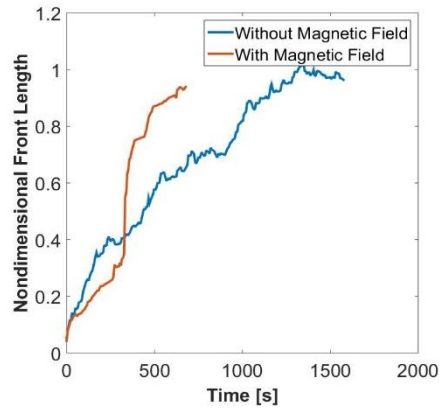
The observations from this laboratory scale experiments have ramifications in various fields. The characteristic property of ferrofluids to get magnetized when a magnetic field is exerted can be utilized to trace the targeted zones in the subsurface. They can be used for displacement of more viscous fluids in a system without being in direct contact to it. The predictable final configuration of the ferrofluids around the magnet makes it a viable application in the field of engineering. The experiments laid out in this thesis were designed to control the displacement of ferrofluid in a porous medium. The observations can be summarized:

- Ferrofluids solely move through the porous media in a predictable final configuration because of the magnetic field, and the experimental observations state the heterogeneities do not affect the flow path of ferrofluids.
- Ferrofluids can displace a more viscous fluid under the effect of magnetic field.
- Flow of ferrofluid due to magnetic field in turn is unstable.
- The experimental and post processed image analysis demonstrate that the finger formation gets suppressed with ferrofluid, because the magnetic field out pulls the viscosity forces and the surface tension acting on the fluid.

The graphs shown in the image is for ferrofluid injection in an air and oil saturated medium at flow rates of 1 and 6, which relates to 126microlitres/min and 23.4microlitres/min respectively. The blue line represents the length covered without a magnetic field and the red represents the length covered when a magnetic field was in place. The perimeter vs time curve for ferrofluid injection into an air and oil saturated medium shows, the effect of magnetic field and no magnetic field on the displacement of Oil and air when ferrofluid is the working fluid. The length covered by ferrofluid when injected in an oil saturated medium is more when a magnetic force was implied. The perimeter of ferrofluid when a magnetic field is in the vicinity is about 1cm at 102 secs and with no magnetic force is less than 0.5 cm. The accelerated motion supports the objective, that the fluid motion can be controlled.

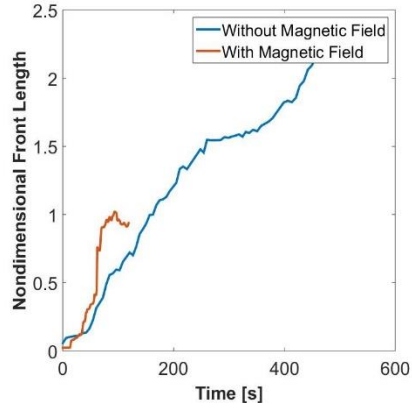


(a) U1

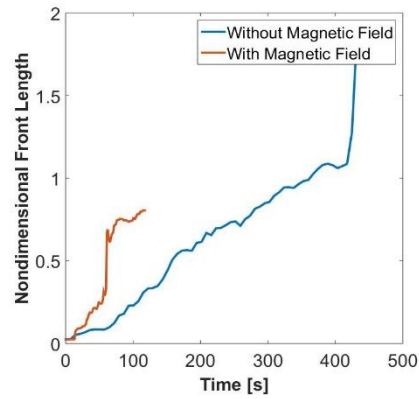


(b) U6

Figure 4.1: Perimeter vs Time curve for ferrofluid injection into an Oil saturated medium at flow rates 126microlitres/min and 23.4 microliters/min (U1 and U6 respectively) with or without the magnetic field in vicinity



(a) U1



(b) U6

Figure 4.2: Perimeter vs Time curve for ferrofluid injection into an air saturated medium at flow rates 126microlitres/min and 23.4 microliters/min (U1 and U6 respectively) with or without the magnetic field in vicinity

4.3 Future Work

The experimental results are up to date with the laboratory scale analysis. Further investigation and large scale experimentation can help quantify the effective displacement of ferrofluids in a subsurface. Further research into quantifying the volume of oil displaced can find an immediate application in oil recovery techniques. The length scales at which the decline in magnetic strength takes place is one of the limitations. As the decline in strength is quite high with increasing distance. More research into this issue would increase the application of ferrofluids for longer length scales applications.

5. Bibliography

[1]S. E. Borglin, G. J. Morikis, and C. M. Oldenburg. Experimental studies of the flow of ferrofluid in porous media. *Transport in Porous Media*, 41(1):61–80, 2000.

[2]Christophe Cottin, Hugues Bodiguel, and Annie Colin. From Capillary Fingering to Viscous Flow in Two-Dimensional Porous Media: Role of the Wetting Properties. Pages 1–2.

[3]Li Dongqing. Encyclopedia of microfluidics and nanofluidics @ONLINE, December 2015.

[4]Francis A. L. Dullien. Two-phase flow in porous media. *Chemical Engineering & Technology*, 11(1):407–424, 1988.

[5]M Ferer, Grant S Bromhal, and Duane H Smith. Two-phase flow in porous media: Crossover from capillary fingering to compact invasion. *Developments in Water Science*, 55(PART 1):153–161, 2004.

[6]Frederick M Fowkes. Attractive forces at interfaces. *Industrial & Engineering Chemistry*, 56(12):40–52, 1964.

[7]Practical Guide, Fluid Flow, Porous Media, Home About, Fundamentals How, To Applications, and Workshop Opportunities. *A Practical Guide to Fluid Flow in Porous Media*. Pages 3–5, 2016.

[8]S. Gupta and A. Pramanik. Torsional surface waves in an inhomogeneous layer over a fluid saturated porous half-space. *Journal of Mechanics*, 32:113–121, 2 2016

[9]Vladimir Gurau, Michael J. Bluemle, Emory S. De Castro, Yu-Min Tsou, J. Adin Mann, and Thomas a. Zawodzinski. Characterization of transport properties in gas diffusion layers for proton exchange membrane fuel cells. *Journal of Power Sources*, 160(2):1156–1162, 2006. [10]G M Homsy. Viscous Fingering in Porous Media. *Annu. Rev Fluid Mech.*, 19:271–311, 1987.

[11]Bhavna; Chandak Krishna Bijay; Iyer Venkat; Mahajan Hrishikesh Prakash Kothari, Nikita; Raina. Application of Ferrofluids for Enhanced Surfactant Flooding In IOR. Society of Petroleum Engineers, 2010.

[12]Roland Lenormand, Eric Touboul, and Cesar Zarcone. Numerical models and experiments on immiscible displacements in porous media, 1988.

[13]M Levy, I Illic, R Scarmozzino, R M Osgood, R Wolfe, C J Gutierrez, and G A Prinz. Thin-Film-Magnet Magneto-optic Waveguide T. 5(2):198–200, 1993.

[14]M Levy, R Scarmozzino, R M Osgood Jr, R Wolfe, F J Cadieu, H Hegde, C J Gutierrez, M Levy, R Scarmozzino, and R M Osgood. Permanent magnet film magneto optic waveguide isolator Permanent magnet film magneto-optic waveguide isolator. 6286(1994):25–28, 1995.

[15]L B N Lf, Ernest Orlando Lawrence, Sharon E Borglin, and George J Moridis. Experimental Studies of Magnetically Driven Flow of Ferrofluids in Porous Media Earth Sciences Division. (August), 1998.

[16]E F Medici and J S Allen. Existence of the phase drainage diagram in proton exchange membrane fuel cell fibrous diffusion media. Journal of Power Sources, 191(2):417–427, 2009.

[17]E F M'edici and J S Allen. Scaling percolation in thin porous layers. Physics of Fluids, 23(12), 2011.

[18]Ezequiel F M'edici. Water Transport in Complex, Non-Wetting Porous Layers with Applications to Water Management in Low Temperature Fuel Cells. 2010.

[19]Saber Mohammadi, Mohammad Hossein Ghazanfari, and Mohsen Masihi.

A pore-level screening study on miscible/immiscible displacements in heterogeneous models. Journal of Petroleum Science and Engineering, 110:40– 54, 2013.

[20]Cm Oldenburg, Se Borglin, and Gj Moridis. Numerical simulation of ferrofluid flow for subsurface environmental engineering applications. Transport in Porous Media, (m):319–344, 2000.

- [21]D Paradis. Difference between paramagnetism and ferromagnetism @ON- LINE, July 2012.
- [22]P. G. Saffman and Geoffrey Taylor. The penetration of a fluid into a porous medium or Hele-shaw cell containing a more viscous liquid. *Proceedings of the Royal Society of London A: Mathematical, Physical and Engineering Sciences*, 245(1242):312–329, 1958.
- [23]K C Sahu, H Ding, P Valluri, and O K Matar. Pressure-driven miscible two-fluid channel flow with density gradients. Pages 1–29, 2008.
- [24]J I Siddique, D M Anderson, and Andrei Bondarev. Capillary rise of a liquid into a deformable porous material. (December 2008):1–15, 2009.
- [25]Saleem Qadir Tunio, Abdul Haque Tunio Mehran, Naveed Ahmed Ghirano, and Ziad Mohamed El Adawy. Comparison of Different Enhanced Oil Recovery Techniques for Better Oil Productivity. *International Journal of Applied Science and Technology*, 1(5):143–153, 2011.
- [26]D Wilkinson and J F Willemsen. Invasion percolation: a new form of percolation theory. *Journal of Physics A: Mathematical and General*, 16(14):3365–3376, 1999.
- [27]Zhiwei Wu, Xiang'an Yue, Tao Cheng, Jie Yu, and Heng Yang. Effect of viscosity and interfacial tension of surfactant-polymer flooding on oil recovery in high-temperature and high-salinity reservoirs. *Journal of Petroleum Exploration and Production Technology*, 4(1):9–16, 2014.
- [28]Changyong Zhang, Mart Oostrom, Thomas W. Wietsma, Jay W. Grate, and Marvin G. Warner. Influence of viscous and capillary forces on immiscible fluid displacement: Pore-scale experimental study in a water-wet micromodel demonstrating viscous and capillary fingering. *Energy and Fuels*, 25(8):3493–3505, 2011.
- [29]Minyao Zhou. Immiscible-Fluid the Contact-line. 45(8), 1992.
- [30]Gui Ping Zhu, Nam Trung Nguyen, R. V. Ramanujan, and Xiao Yang Huang. Nonlinear deformation of a ferrofluid droplet in a uniform magnetic field. *Langmuir*, 27(24):14834–14841, 2011.
- [31]P Zitha, R Felder, D Zornes, K Brown, and K Mohanty. Increasing Hydrocarbon Recovery Factors. *The Society of Petroleum*, pages 1–9, 2008.